Robust Estimation of Pulse Transit Time Difference from Photoplethysmographic Signals

Estimación robusta de la diferencia del tiempo de tránsito del pulso sanguíneo a partir de señales fotopletismográficas

AUTHOR: PABLO ARMAÑAC JULIÁN

Master's Degree in Biomedical Engineering
TRABAJO DE FIN DE MÁSTER , UNIVERSIDAD DE ZARAGOZA

DIRECTOR: SPYRIDON KONTAXIS
CO-DIRECTOR: EDUARDO GIL HERRANDO

DECLARACIÓN DE AUTORÍA Y ORIGINALIDAD

(Este documento debe acompañar al Trabajo Fin de Grado (TFG)/Trabajo Fin de Máster (TFM) cuando sea depositado para su evaluación).

TRABAJOS DE FIN DE GRADO / FIN DE MÁSTER

D./Dª. PABLO ARMAÑAC JULIÁN ,

con nº de DNI 76919485X en aplicación de lo dispuesto en el art. 14 (Derechos de autor) del Acuerdo de 11 de septiembre de 2014, del Consejo de Gobierno, por el que se aprueba el Reglamento de los TFG y TFM de la Universidad de Zaragoza,

Declaro que el presente Trabajo de Fin de (Grado/Máster) MÁSTER , (Título del Trabajo) ESTIMACIÓN ROBUSTA DE LA DIFERENCIA DEL TIEMPO DE TRÁNSITO DE PULSO SANGUÍNEO A PARTIR DE SEÑALES FOTOPLETISMOGRÁFICAS,

ROBUST ESTIMATION OF THE PULSE TRANSIT TIME DIFFERENCE FROM PHOTOPLETHYSMOGRAPHIC SIGNALS

,

es de mi autoría y es original, no habiéndose utilizado fuente sin ser citada debidamente.

Zaragoza, 21/11/2018

Fdo: Pablo Armañac Julián

ABSTRACT

In this work, the possibility of detecting mental stress using non-invasive techniques based on the photoplethysmographic signal (PPG) will be studied. To this end, the aim is to detect changes in arterial pulse wave velocity (PWV), using PPG signals taken at two different points on the arterial tree with which to measure the arrival time of the arterial pulse at the periphery (PAT) and the difference of that arrival time between two different points on the periphery (PTTD). PTTD has been proposed in the literature as a measure correlated with pulse transit time (PTT), the latter capable of measuring changes in cardiovascular dynamics.

Both PAT and PTTD are influenced by PTT but, unlike PAT, PTTD is not influenced by the pre-ejection period (PEP) - a time interval in ventricular systole that changes from pulse to pulse - which causes PAT to lose its relationship with PTT. This beats PTTD in certain applications such as arterial stiffness assessment or non-invasive blood pressure estimation (from PPG), so it will apparently serve our purpose as well.

First, a reliability study of the PPG fiducial points is performed to verify the optimal way to detect PPG pulses with the highest precision. It is demonstrated by various analyses that the best point to detect the pulses corresponds to the value of the PPG at the moment of maximum slope (maximum value in the first derivative). It is necessary to implement an artefact detector since the method of acquisition of the PPG is very sensitive to them and there may be segments in which the recorded signal is absolutely useless.

Subsequently, fourteen healthy volunteers undergoing a stress protocol are analysed and a statistical test is carried out to check the validity of the proposed method. The results show that the standard deviation of the PTTD has sufficient statistical capacity to discern between states of stress and relaxation, for each of the subjects separately. Furthermore, a generalised descending trend of the mean PTTD can be seen in stress with respect to relaxation.

By way of conclusion, it has been found that PTTD contains physiological information that may be of interest for stress detection. In turn, it is also a potentially interesting technique for other types of clinical applications such as non-invasive blood pressure estimation or arterial stiffness assessment, but the adequacy of arterial stiffness in each particular scenario needs to be studied. In addition, as PTTD can be measured from only two PPG signals, the technique is suitable for wearable and smartphone devices.

Keywords: Autonomic Nervous System; Sympathovagal Balance; Non-invasive Monitoring; Stress; Photoplethysmography; PPG; Pulse Transit Time; Pulse Transit Time Difference;

RESUMEN

En el presente trabajo se va a estudiar la posibilidad de detectar estrés mental utilizando técnicas no invasivas basadas en la señal fotopletismográfica de pulso (PPG). Para ello se pretende detectar cambios en la velocidad de pulso arterial (PWV), utilizando señales de PPG tomadas en dos puntos distintos del árbol arterial con las que poder medir el tiempo de llegada de pulso arterial a la periferia (PAT) y la diferencia de ese tiempo de llegada entre dos puntos de la periferia distintos (PTTD).

Tanto el PAT como el PTTD han sido propuestas en la bibliografía como medidas influenciados por el Tiempo de Tránsito de Pulso (PTT), este último capaz de medir cambios en la dinámica cardiovascular. Sin embargo, el PTTD, al contrario que el PAT, no necesita del electrocardiograma (ECG) para ser obtenido y no está influenciado por el periodo de pre-eyección (PEP) -un intervalo de tiempo en la sístole ventricular que cambia pulso a pulso- el cual genera que el PAT pierda la relación con el PTT, dos factores importantes que aventajan al PTTD frente al PAT.

Primero, se estudia de fiabilidad de los puntos fiduciales para la detección de los pulsos de la señal PPG y con ésto comprobar cuál es el método con la mayor precisión. Se demuestra mediante diversos análisis que el mejor punto para detectar los pulsos corresponde al valor de la PPG en el instante de máxima pendiente (valor máximo en la primera derivada). Resulta necesario implementar un detector de artefactos ya que el método de adquisición de la PPG es muy sensible a ellos pudiendo llegar a haber segmentos en los que la señal registrada es absolutamente inutilizable.

Posteriormente, se analizan 14 voluntarios sanos sometidos a un protocolo de estrés y se realiza un test estadístico para comprobar la validez del método propuesto. Los resultados muestran que la desviación estándar de la PTTD tiene la capacidad estadística suficiente como para discernir entre estados de estrés y de relajación, para cada uno de los sujetos por separado. Además, se puede ver una tendencia descendente generalizada del descenso de la PTTD en situación de estrés con respecto a relajación.

A modo de conclusión, se ha visto que la PTTD contiene información fisiológica que puede ser interesante para la detección de estrés. A su vez, también es una técnica potencialmente interesante para otros tipos de aplicaciones clínicas tales como la estimación no invasiva de la presión arterial o la evaluación de la rigidez arterial, pero se necesita estudiar la adecuación de ésta en cada escenario en particular. Además, como la PTTD se puede medir a partir de únicamente dos señales PPG, la técnica es idónea para dispositivos *wearable* y *smartphones.*

Palabras Clave: Sistema Nervioso Autónomo; Balance Simpático-Vagal; Monitorización No Invasiva; Estrés; Fotopletismografía; PPG; Pulse Transit Time; Pulse Transit Time Difference;

Acknowledgements

El Trabajo de Fin de Máster (TFM) que nos ocupa se ha desarrollado en colaboración con el grupo BSICoS (Biomedial Signal Interpretation and Computational Simulation), perteneciente al Instituto de Investigación en Ingeniería de Aragón (I3A) de la Universidad de Zaragoza, al Instituto de Investigación Sanitaria de Aragón (IIS Aragón) y al Centro de Investigación Biomédica en Red en Bioingeniería, Biomateriales y Nanomedicina (CIBER-BBN).

Todo el proceso de desarrollo y validación se ha llevado a cabo bajo la supervisión de Spyridon Kontaxis, estudiante PhD en esta misma universidad, con amplia experiencia en la fisiología del estrés y procesado de señales biomédicas, quien ha trabajado sobre la base de datos en la que sustentarán los resultados del TFM; y el Doctor Eduardo Gil Herrando, profesor del Departamento de Informática e Ingeniería de Sistemas (área de Ingeniería de Sistemas Automáticos) de la Universidad de Zaragoza, que ha dirigido la parte de procesado de la señal específica de la fotopletismografía, campo en el que posee amplia experiencia. Por otro lado, también han colaborado ampliamente en la idea principal del estudio y en la discusión y análisis de los resultados Pablo Laguna, Jesús Lázaro y, en especial, Raquel Bailón. Agradecer a todos el buen trato y la atención prestada, además del carácter motivador de todos ellos.

Table of Contents

Introduction

Contents

1.1 Context and Motivation

The autonomic nervous system (ANS) is responsible for regulating, among others, both the cardiac pulse and the constriction of the blood vessels. The inhibition or activation of the sympathetic branch of ANS can cause changes in the speed of the blood as it passes through the arterial tree. Stressful or disturbing stimuli originate an imbalance in that ANS-mediated regulation, thus arising changes in the physiological homoeostasis and cardiovascular dynamics.

Stress can be seen as a physiological process of the human body with a non-specific response [1]. The body reaction in the presence of stress is usually associated with the well-known physiological symptoms like dry mouth, palpitations, muscular tension, brain activity and

sweating. However, many factors, including those about personality, modulate the perception of that stress and the excitement they cause to each person in particular leading to a highly subjective phenomenon. When stress is prolonged or repetitive, it has been associated with psychic and somatic diseases. Moreover, chronic stress has been related to higher risk of suffering cardiovascular diseases.

The World Health Organisation has considered stress as a worldwide epidemic, estimating that 40% of adults aged 25 years and older have been diagnosed with high blood pressure as a consequence. It is perceived as a serious health condition [2] and there are research evidences that acute mental stress has a prolonged unfavorable effect on arterial stiffness [3].

Then, several studies have proposed physiological biomarkers in an attempt to obtain a quantifiable measure of stress including blood pressure (BP), heart rate (HR), various indexes of heart rate variability (HRV) or respiration [4]. Although they are promising, there are still many challenges ahead for the extensive clinical application (the accuracy is one of the key issues to address).

Nowadays, methods exploiting features derived from the photoplethysmographic (PPG) signal can provide continuous cardiovascular information [5], and non-invasive blood pressure estimation [6–9]. However, these techniques do not rely exclusively upon the PPG signal since the electrocardiogram (ECG) is also needed to define the actual PPG-based surrogates of BP measuring.

The possibility of quantifying changes in the sympathovagal balance caused by acute mental stress will be studied in this work, using non-invasive sensors based on PPG and without the need of either the ECG or cuff/intra-arterial BP sensors. This seems appealing considering the current trend of using devices such as smartwatches with the ability to run this type of application in real time [10] and to get a more comfortable procedure for the user allowing a greater ease of assembly of the equipment.

1.2   Physiological Aspects

In this section, some aspects will be briefly explained in order to understand the physiologic mechanisms involved in the stress response.

1.2.1   Autonomic Nervous System

The brain and the spinal cord compose the central nervous system. A large segment of the nervous system operates at a subconscious level and it is the so-called ANS. It controls many functions of the internal organs, movements of the gastrointestinal tract, secretion by many of the glands of the body and the level of pumping activity by the heart [11].

ANS is composed of two branches (see Figure 1.1). On one hand, the sympathetic nervous system (SNS) "activates" the body in an alarm or stress situation, leading to the so-called fight or flight reaction. The effects of a SNS excitation commonly generates a mass response [11] e.g. heart rate increase, brain activity and vasoconstriction of the vessels among others processes -see Figure 1.2.

On the other hand, the parasympathetic nervous system (PNS) "relaxes" the body and it is responsible of the so-called rest and digest response. A PNS activation mainly produces a decrease in the heart rate and the contractility of the heart but an increase in the intestinal and gland activity. The PNS branch acts in a much more specific way than the SNS branch. For instance, the cardiovascular control of the parasympathetic system only takes effect on the heart rate [11].
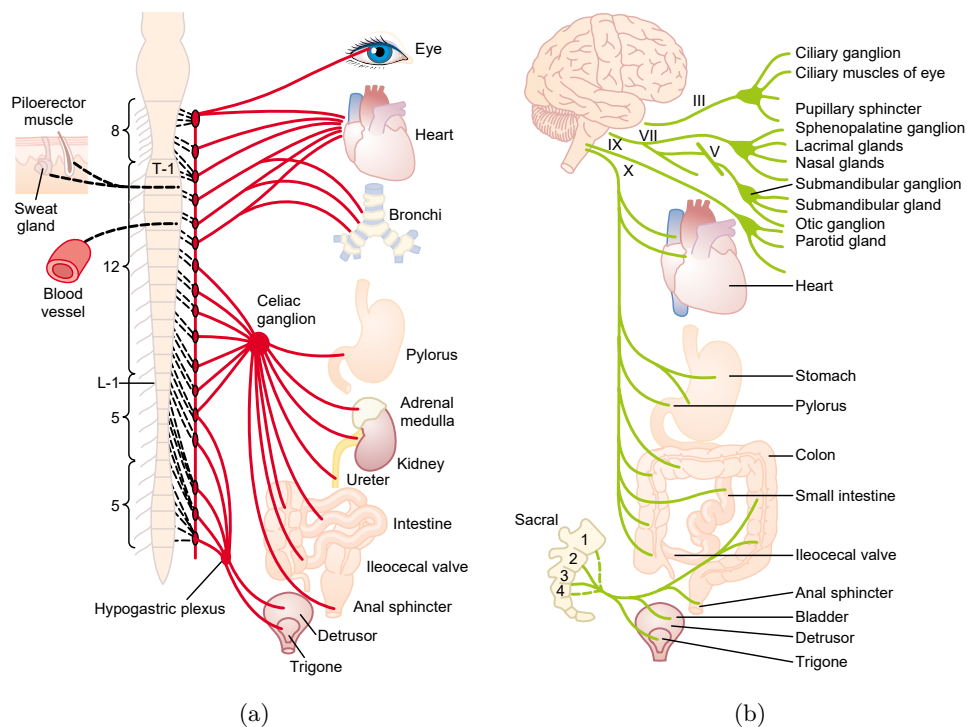

FIGURE 1.1: *Autonomic Nervous System: (a) Sympathetic branch. (b) Parasympathetic branch. Figure reproduced from [11].*

Both branches of the ANS act in a reciprocal manner [12]: increases in the activity of one of them are associated with decreases in the activity of the other one. In this way, the overall status of the organism depends on which ANS branch is predominating and how big this predominance is at each moment. This sympathetic-parasympathetic balance is commonly referred to as sympathovagal balance. However, some processes are known to be controlled by only one of the branches, e.g. respiration is controlled by only the parasympathetic branch and arteries constriction is controlled only by the sympathetic branch.
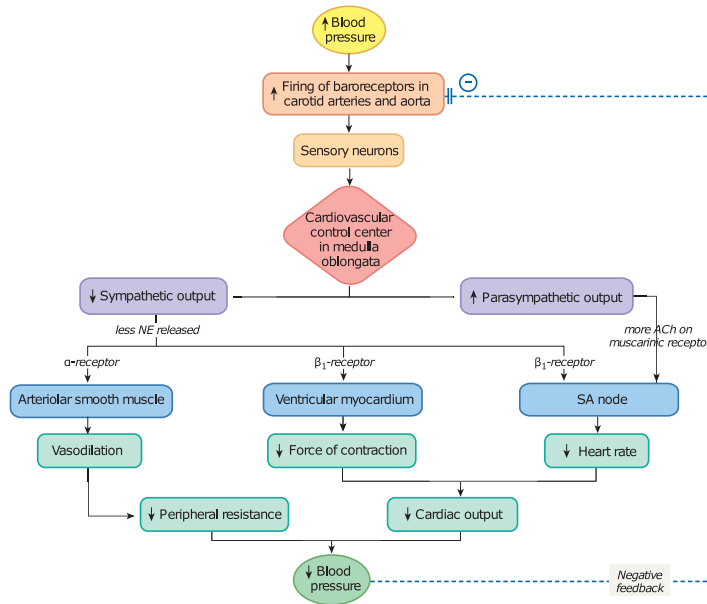
FIGURE 1.2: *Cardiovascular Regulation. Figure reproduced from [13].*

An increase in the SNS activity results in an increase of the BP mediated by 3 main processes (see Eq. 1.1):

1. Vasoconstriction in all arterioles, raising the Total Peripheral Resistance (TPR).
2. Vasoconstriction of the veins, then injecting a high amount of blood volume, raising the Venous Return (VR) and consequently increased filling of the left ventricle (also known as preload or end-diastolic volume) and increased Cardiac Output (CO).
3. High stimulation of the sinoatrial node, increasing the heart rate and the CO.

1.2.2   Pulse Rate Variability

Heart Rate Variability (HRV) analysis, or Pulse Rate Variablity (PRV) when referring to pulse-derived signals, attempts to assess cardiac autonomic regulation through quantification of sinus rhythm variability. HRV has received, in recent years, widespread research interest since the state of the autonomic nervous system, and related diseases, can be investigated non-invasively with an ECG using relatively simple signal processing techniques.

The analysis of HRV is based on the series of occurrence times originally produced by the QRS. Despite the seeming simplicity of deriving the series of RR intervals (time intervals between successive heartbeats) from the ECG signal or pulse-to-pulse from the PPG signal, it is nonetheless absolutely essential to assure that HRV is analysed accurately with the presence of any supra-ventricular ectopic beats, false/missed normal beat detections or fiducial point misalignment [14].

Clinical studies focused on heart diseases have sometimes been synonymous with the use of

HRV (see Task Force for further information [15]). Physiological information may be inferred by quantifying the power spectral density of the different frequency components to determine various pathologies or physiological states related to cardiac autonomic function. The spectral estimation of the HRV is characterized by two main components: the low frequency (LF) component, defined in [0.04, 0.15] Hz, and the high frequency (HF) component, defined in [0.15, 0.4] Hz. The power in the HF band is considered a measure of PNS activity, mainly related to respiration through respiratory sinus arrhythmia, and the power in the LF band is considered a measure of both SNS and PNS activity.
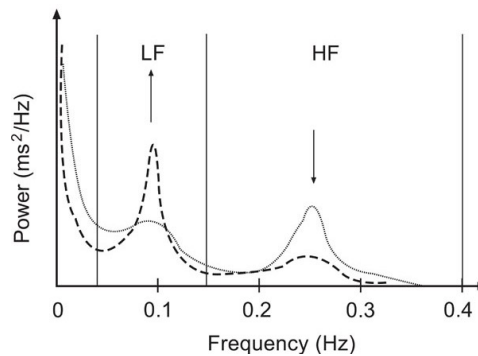

FIGURE 1.3: *HRV spectral estimation during tilt-rest protocol (dashed line - dotted line respectively). Tilt is associated with SNS activity and rest with PNS activity.*

1.2.3 Human Stress Response

The response of the ANS to a stressful stimulus is characterized by an inhibition of the PNS and consequently an activation of the SNS (fight-or-flight response). Both systems act in opposite ways generating activity to the adrenal medulla that is reflected by the increase of heart rate, blood pressure, broncho-dilation, sweating, metabolic activity and blood glucose concentration [16].

Before a stressful stimulus, it is perceived by the sensory system and a warning signal is transmitted to the hypothalamus, where the arousal of two systems is generated as consequence: the hypothalamic-pituitary-adrenal (HPA) axis and the SNS branch of the ANS.

- State of alertness or excitement together with inflammatory processes and immune responses.
- Increase in temperature and respiratory rate for the elimination of toxins.
- Increase in gluconeogenesis and lipolysis offering oxygen, nutrients and energy to the tissues to increase attention and concentration.
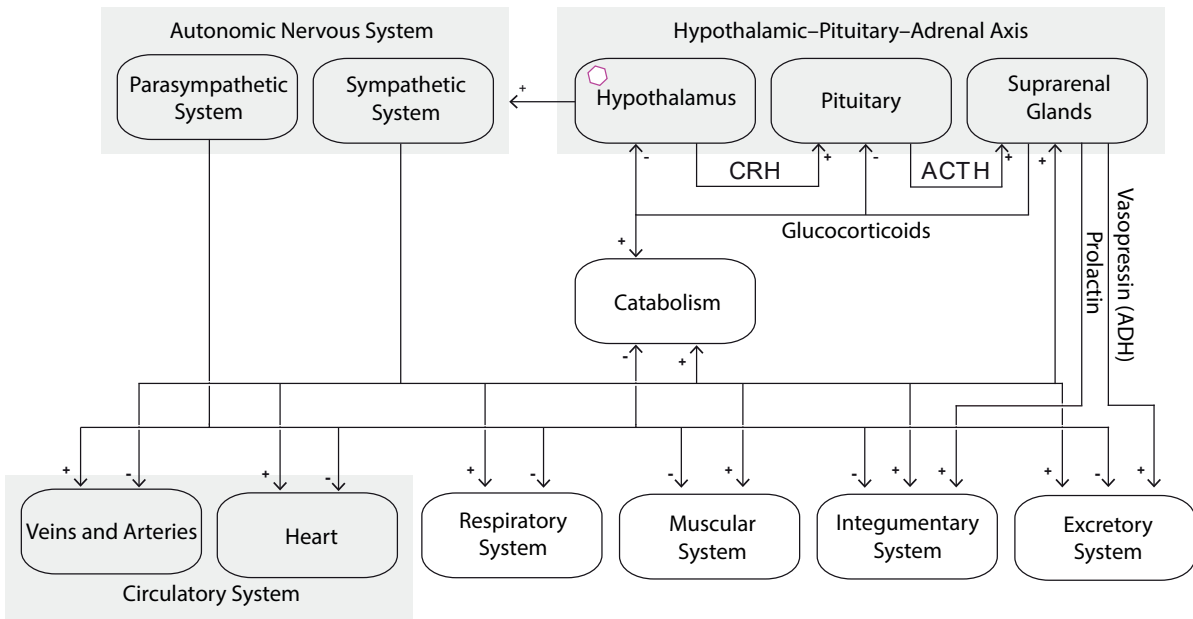
FIGURE 1.4: *Neuroendocrine activations that take place in response to stress. The white circle in the Hypothalamus represents the performance of the stressful stimulus. CRH and ACTH stand for Corticotropin-releasing hormone and Adrenocorticotropic hormone respectively. Figure reproduced from [17].*

Cortisol is a glucocorticoid hormone indirectly segregated by an HPA axis activation and its free portion generally acts by activating the catabolic pathways with a life expectancy of 60-90 minutes in circulation. The activation of the HPA axis and the ANS happens simultaneously. However, the effects of the HPA axis take the order of minutes to be reflected in the body, as opposed to the effects caused by the activation of the ANS that happens instantaneously. So, the latter system activation will be the only one analysed and studied in this work. Figure 1.4 shows the interaction of the different systems involved in the neuro-endocrine response of stress [18].

1.3   Pulse Photoplethysmographic Signal

Photoplethysmography is a technique introduced by Hertzman [19] which allows to measure blood volume variations in the microvascular bed of tissue. PPG makes use of low-intensity infrared light and red light wavelength. When this light travels through biological tissues it is absorbed by bones, skin pigments and both venous and arterial blood. Since light is more strongly absorbed by blood than the surrounding tissues, the changes in blood flow can be detected by PPG sensors as changes in the received intensity of light[1]. The voltage signal from a PPG sensor is proportional to the quantity of blood flowing through the blood vessels.

The PPG signal has two components: one reflecting the arterial pulse produced by the heartbeats (AC component), and another due to the non-pulsating blood volume and the surrounding

---

[1]Blood flow variations mostly occur in the arteries and not in the veins.
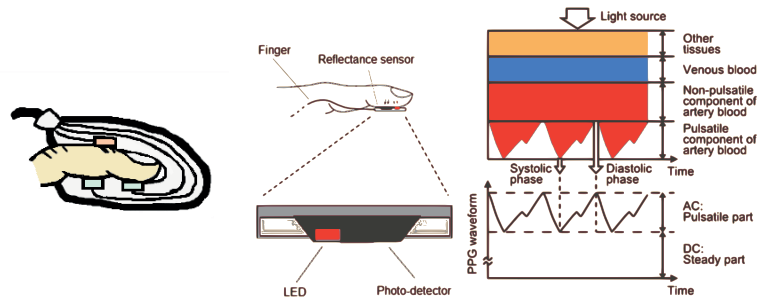
FIGURE 1.5: *PPG optical technique and fundamentals. Figure reproduced from [20].*

tissue producing a signal with slow changes (DC component) -see Figure 1.5. The latter arises from the optical signals reflected or transmitted by the tissues as well as venous and arterial blood volumes. The basic frequency of the AC component varies with the heart rate and is superimposed on the DC baseline. The AC-component of the PPG waveform is normally flipped horizontally just for computation. Figure 1.6 shows morphology of PPG pulses from 2 subjects in ears, fingers, and toes.
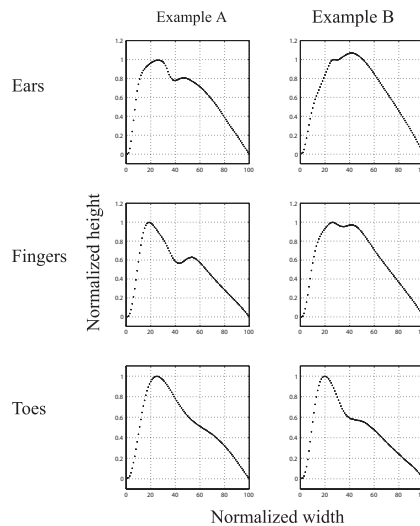

FIGURE 1.6: *Morphology examples for two different healthy subjects, contour of the PPG. Figure reproduced form [21].*

The morphology of the AC-component in the PPG pulses can be divided into two phases: on one hand, the rise of the pulse (anacrotic phase) which corresponds to the ventricular systole and on the other hand, the descent of the pulse (catacrotic phase) which corresponds to the ventricular diastole and the wave reflections from the periphery. A dicrotic notch (see figure 1.7), is usually seen in the catacrotic phase of subjects with healthy compliant arteries and is said to indicate the closure of the semilunar aortic valve and pressure wave reflections.

Photoplethysmography-based techniques have been proposed for many clinical settings and applications such as physiological monitoring, vascular assessment and ANS study [22]. Nevertheless, the most clinically adopted PPG-based device is the pulse oximeter, which is mainly
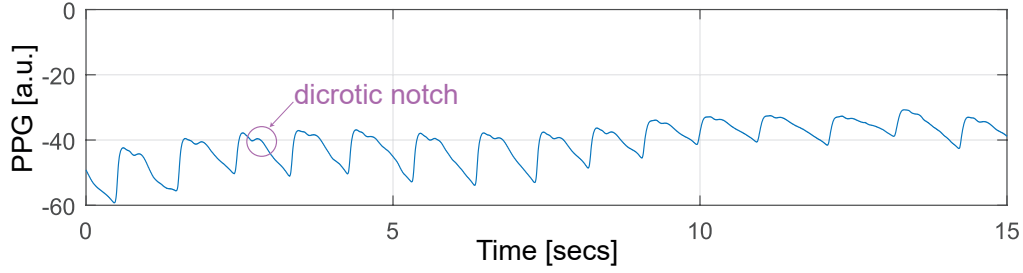
FIGURE 1.7: *Example of PPG signal.*

used to monitor the peripheral oxygen saturation (SpO_2) and the pulse rate (PR). Vasoconstriction events can be detected with PPG-based techniques by decreases in the signal amplitude fluctuation [23, 24] and have been proposed for obstructive sleep apnea syndrome (OSAS) screening [25, 26].

1.4   Methodological Aspects

The applied methodology is based on the physical concepts regarding fluid velocity throughout a tube in a laminar regime without turbulence (Hagen-Poiseuille law, Continuity equation and Ohm's law). The latter is the most important to take into account and reads:

$$BP \; = \; CO \; * \; TPR, \tag{1.1}$$

where:

- CO = Cardiac Output
- TPR = Total Peripheral Resistance

In biomechanics, the Moens–Korteweg equation models the relationship between pulse wave velocity (PWV) and the incremental elastic modulus of the arterial wall or its distensibility [27, 28]. It is derived from Newton's second law of motion for a long straight elastic tube and reads:

$$PWV \; = \; \frac{L}{PTT} \; = \; \sqrt{\frac{E_{inc} \; \cdot \; h}{\rho \; 2 \; r}}, \tag{1.2}$$

where:

- L = Distance between two points of the arterial tree
- PTT = Pulse Transit Time
- E = Incremental Young Elasticity Modulus of the Vessel Wall
- h = Constant ratio of Wall Thickness
- ρ = Blood Density
- r = Vessel Radius

Equation 1.2 has been written under quite restrictive assumptions of a homogeneous arterial segment and requires in practice two pulse detectors to be accurately positioned on the arterial tree to be measured. A change in the sympathovagal balance -seen as a change in the blood vessels' properties: vascular radius, compliance and thickness- will produce a change in the PTT, hence PWV.

1.4.1 Pulse Transit Time (PTT)

PTT stands for the time that the pressure wave takes to propagate between two points of the arterial branch. The speed at which this arterial pressure wave travels is directly proportional to blood pressure.

There is no published comparison between PTT and stress response. However, the Oxford team has reported a comparison between PTT values and non-invasive measurement of blood pressure using "Finapres" validating that it is inversely proportional to BP [29]. However, results showed that absolute values of PTT cannot be extrapolated as absolute values of blood pressure at a given point in time, but it is capable of predicting changes in blood pressure over a short period of time [5].

Hence, PTT represents a tool for assessing arterial stiffness (as derived in Equation 1.2), and it also seems to be the best basis for a non-invasive-ubiquitous-cuff-less BP monitor [7]. Two points of the arterial tree are needed for the PTT computation: a proximal and a distal point.

1.4.2 Pulse Arrival Time (PAT)

PAT is the time it takes the pulse pressure waveform to propagate through the arterial vessels from the heart to the periphery. It can be measured as the time delay between two points: the proximal one defined using an ECG signal and the distal point defined using any waveform signal able to measure cardiovascular changes. The most popular technique involves the one-lead R-peak of the QRS complex and the PPG clip at a finger, toe, forehead or ear. The R peak provides the start time of each heartbeat and the PPG volume pulse determines the arrival time.

PTT is the true transit time of the pulse along the arterial wall over a long non-homogeneous vascular path rather than the PAT [30–34], as PAT definition leads to an estimation of the transit time made up of two parts (see also Figure 1.8):

$$PAT = PEP + PTT \tag{1.3}$$

Figure 1.8 exhibits that when using the R-peak at the ECG, PAT is not exactly the PTT as it includes the time interval between ventricular depolarization (taken as the R-wave peak
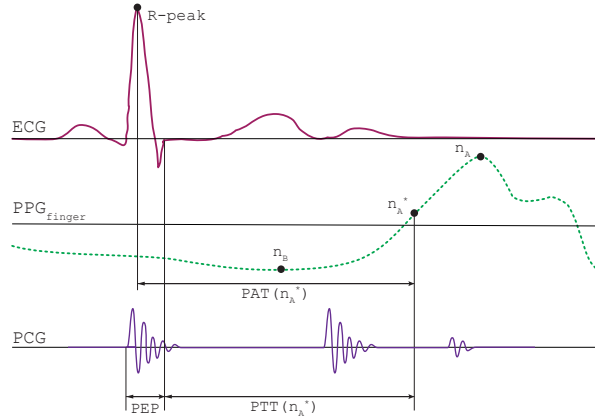
FIGURE 1.8: *Difference between PAT and PTT caused by PEP (measured with phonocardiography(PCG)).*

occurrence) and the opening of the aortic valve (PEP or isometric contraction), which varies beat-to-beat.

The use of the name PTT instead of PAT is a common mistake made in the literature and the extracted results obtained by using the PAT technique are not purely correct as they include PEP (see Eq. 1.4) [7, 35, 36].

$$PWV \simeq \frac{L}{PEP + PTT} < \frac{L}{PTT} \tag{1.4}$$

1.4.3   Pre-Ejection Period (PEP)

There is a small delay between the ventricular depolarization and the opening of the aortic valve known as isovolumic contraction time or PEP. The QRS complex is associated with the onset of ventricular contraction, but this contraction continues for a period of time until sufficient pressure is generated in the left ventricle to force the opening of the aortic valve and the exit of the blood flow.

Isovolumic contraction, the first phase of systole, begins when myocyte contraction increases ventricular wall stress. The rising intraventricular pressure closes the mitral valve, after which pressure increases until it exceeds that in the aorta, which causes the aortic valve to open. Until this happens, blood can neither enter nor leave the ventricle so that the increase of pressure at a constant volume inscribes an upward deflection. The second phase, *ejection*, begins when ventricular pressure exceeds that in the aorta, after which blood is pumped into the aorta. Systole ends when the loop reaches the *end-systolic pressure-volume relationship* and diastole begins with *isovolumic relaxation* which occurs after aortic valve closure[37].

PEP is significantly affected by the heart inotropy and can also be regarded as an index of
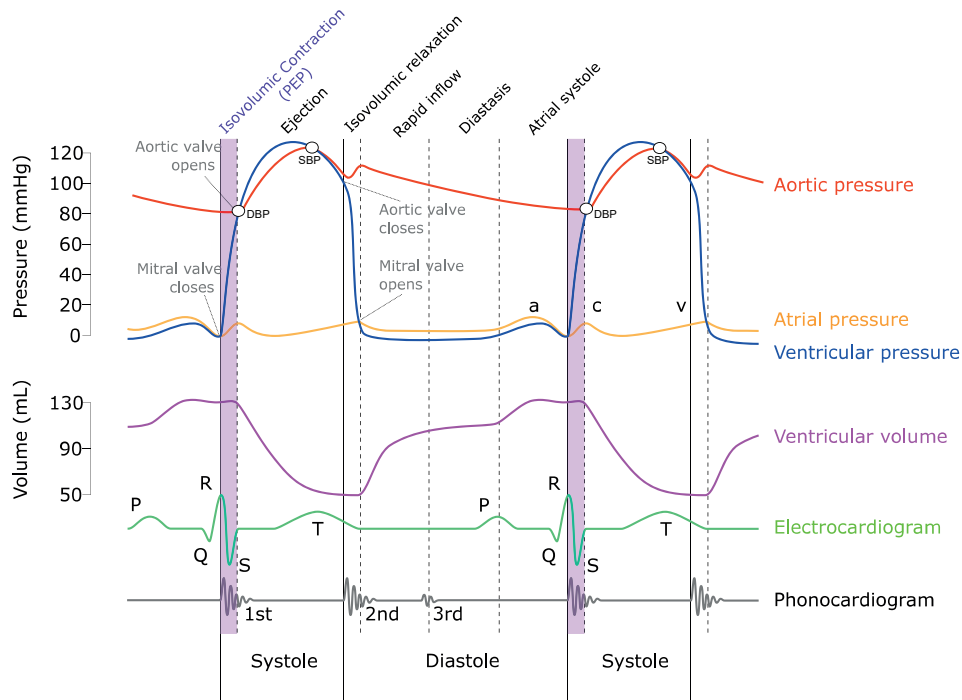
FIGURE 1.9: *The Pre-Ejection Period in shaded purple; Wiggers Diagram.*

cardiac sympathetic (β-adrenergic) activity. While the electromechanical delay (also kwonw as refractory period) in healthy human takes 30–40 milliseconds, the duration of isometric contraction is more variable [38].

To sum up, the higher the heart rate, the lower the PEP is expected, observation demonstrated in [39]. Enhance that PEP is a non-constant effect that produces non-measurable variations in PAT using only an ECG and a PPG signal. On the contrary, a few studies indicated that PTT with PEP included actually have a better performance for BP estimation than removing the PEP [40], which demonstrates the possible positive effect of PEP in BP estimation and the discrepancies in the literature regarding this effect.

As influences of the vascular or vasomotor tone in the PEP make PAT more inconvenient than the PTT for arterial stiffness assessment [35] or blood pressure estimation[7, 36], some alternatives to ECG for measuring the proximal point [7], including ballistocardiography, seismocardiography, impedance-cardiography (ICG) and phonocardiography (PCG) have been proposed. However, the main problems of these techniques are that they require a large quantity of sensors and electrodes and their complexity.

1.4.4   Pulse Transit Time Difference (PTTD)

Other technique to avoid the influence of PEP non-invasively, and using only 2 PPG sensors, is to measure the difference in time between two PPG pulse waves affected by the same PEP; leading to the PTT difference (PTTD). It is worth noting that neither ECG, nor ICG nor PCG

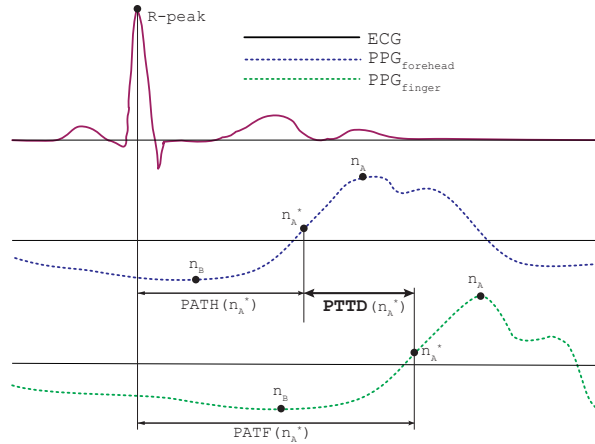are necessary for this technique, but only two PPG sensors.

FIGURE 1.10: *PAT towards the finger (PATF), PAT towards the forehead (PATH) and PTTD definitions.*

Although considerable research has been devoted to PAT for arterial stiffness assessment, rather less attention has been paid to the PTTD [41]. Furthermore, PTTD has been studied as a surrogate of PTT as well [42]. The study in [42] reported an analysis of correlation between PTTD and PAT signals during rest conditions within the whole spectrum, while several modulations with different physiological origins are expected in PTT signals [43, 44]. In [45], an analysis of the correlation between PTTD and PATF dynamics during a tilt table test showed that PTTD is a non-invasive measure potentially correlated with PTT that is not influenced by PEP; an advantage in the applications yet mentioned.

1.5   Objectives and Scope of the project

As commented before, PTT is able to measure changes in blood pressure, and so, our hypothesis was that mental stress could be detected by quantifying the changes induced in the cardiovascular dynamics, seen as changes in PTTD. The main objective of the project is to evaluate the capability of the PTTD, obtained non-invasively from two PPG signals, on detecting mental stress episodes.

Compared to the ECG signal, the PPG waveform is smoother and it is not characterized by a clearly detectable feature [46], making the delineation of the PPG pulses challenging. The selection of the most feasible PPG-sensor location and the measurement technique can be challenging [47]. Peralta et al. [48] have studied different measuring techniques and Fiducial Point (FP) for the ANS evaluation through the PRV signal. Hence, an important first step for the PTTD analysis is the detection of the PPG pulse wave and the FPs definition. In order to define the most accurate FP under artefactual conditions and different PPG morphologies; different FPs for the temporal location of each pulse wave have been studied.

The project is divided into two distinct phases:

1. Reliability analysis of the PPG delineation in artefactual environments.
2. Study of the capability of the PTTD to detect cardiovascular changes evoked by stress.

In the development process of the project, the main points addressed are the following:

i. Review of the State of the Art: cardiovascular physiology through the PPG and ECG.
ii. Preprocessing of the signals implementing the artefact detector and the evaluation of signal quality.
iii. Validation of robustness detection for different fiducial points in PPG signals.
iv. Computation of the PAT and PTTD signals obtained from the forehead and finger in acute mental stress episodes.
v. Discussion of the obtained results and interpretation of the physiological processes.
vi. Feasibility study of the proposed methodology to detect mental stress.

For the development of all the necessary algorithms and sample of results, the MATLAB tool was used: extraction of the PAT towards the forehead (PATH), the PAT towards the finger (PATF) and their difference -the PTTD. A database obtained at *Universidad de Zaragoza* (UZ) will be used to verify the implemented algorithms, in which 40 healthy volunteers performed a experimental protocol based on two sessions: relax and stress.

1.6 Outline of the manuscript

The remainder of this memoir is divided into 3 chapters as follows:

Chapter 2: In this chapter, we address the problems concerning PPG signal quality, and all the developed processing techniques to delineate the PPG waveform in a proper way. So, it concludes with which is the best fiducial point to use in artefactual environments.

Chapter 3: In this chapter, based on the results obtained in Chapter 2, we address how to detect the state of stress using the PTTD methodology, with only two PPG sensors.

Chapter 4: This chapter summarizes the main conclusions of the previous chapters and will present the future work with which to continue the present project.

PPG Fiducial Points Robustness Analysis in Artefactual Environments

Contents

The signal processing stage and the feature extraction of the PPG signals were very important issues to take into account. In this chapter, an algorithm to process the PPG signals in artefactual environments will be defined and then, the robustness analysis of the FP will be investigated.

In previous studies made in this group, the PPG pulses were detected using a published and validated method developed by Lázaro et. al [49]. The basis of the method is to find the systolic slope of the AC component and taking the middle point of that slope. However, in non-stationary

environments, it is necessary to define FPs robust to possible changes in morphology. Another important point is that there is the need to develop an artefact detector in order to suppress bad quality PPG segments where the signal shouldn't be delineated.

In the database used for the analysis, the PPG recorded at the forehead happened to be low-quality signals, with a large amount of artefacts caused by both movements and bad sensor placement. Thus, artefact detection techniques and the selection of the most robust FP should be determined in an automatic manner, before feature extraction for stress assessment.

2.1   Materials

2.1.1   Database

A database of 40 healthy volunteers (half men and half women), not diagnosed with any chronic or psychological disease and with an average age of 21.99 ± 2.87 years, is used. These registrations were done at the Universidad de Zaragoza. The protocol was approved by the Ethics Committee. Also, all the subjects volunteered to participate and gave their informed consent before taking part in this study.

The *ABP 10 module (Medicom 83 system, MTD Ltd, Russia)* was used to record the database, which allows, among other possible measures, the simultaneous and synchronized acquisition of the PPG at both the forehead and the finger sampled at 250 Hz and the ECG by 3 orthogonal leads sampled at 1 KHz. An example of registered signals is shown in Figure 2.3. For the analysis developed in this chapter, the signals were extracted from a basal stage, where subjects were relaxing (see Section 3.1.1 for a complete description of the database used).

2.2   Methods

The PPG signals had many artefacts, so a pre-process was implemented before the pulse detection and analysis. Post-process was also needed to be implemented in order to correct the detections. After that, PAT and PTTD were computed for different FPs and a statistical test was used to decide the most reliable one for PTTD applications.

2.2.1   Signal pre-process

Preprocessing is considered the first phase in signal processing to adjust the recorded signals so that they become more acceptable for feature extraction. The main preprocessing steps, in this project, are the following:

- Filtering
  First of all, the PPG signals are filtered by a bandpass Butterworth Infinite Impulse Response filter ("Forward-Backward" to maintain the morphology of the signals). Baseline contamination was removed from the PPG using a low cut-off frequency of 0.3 Hz, and

high frequency noise was attenuated by a high cut-off frequency of 15 Hz.

- Artefact detection
  After filtering, artefactual PPG pulses were tried to be discarded by using the artefact detector based on Hjorth parameters, described in [25]. They can be used to estimate whether a signal is oscillatory or not. The first Hjorth parameter (H_1) is defined as an estimation of the central frequency of the signal, and the second Hjorth parameter (H_2) as half of the bandwidth. For an intra-subject robustness analysis, a median adaptive filter was implemented using a 3 minutes-length window to define $\widehat{H_1}(n)$ and $\widehat{H_2}(n)$. Empirical thresholds were used to determine whether a signal segment is considered as an artefact under the following conditions:

$$H_1(n) > \widehat{H_1}(n) + T_{1\,up}$$
$$H_1(n) < \widehat{H_1}(n) - T_{1\,low}$$
$$H_2(n) > \widehat{H_2}(n) + T_{2\,up}$$

where $T_{1\,up} = 0.4$ Hz, $T_{1\,low} = 0.4$ Hz, $T_{2\,up} = 1$ Hz for finger and forehead PPG. The Hjorth parameters estimated for one PPG signal are shown in Figures 2.1(b) and 2.1(c). As an example of the artifact detector applicability, one artifact segment detected within the time-interval 535 to 545 seconds is shown in Figure 2.1.
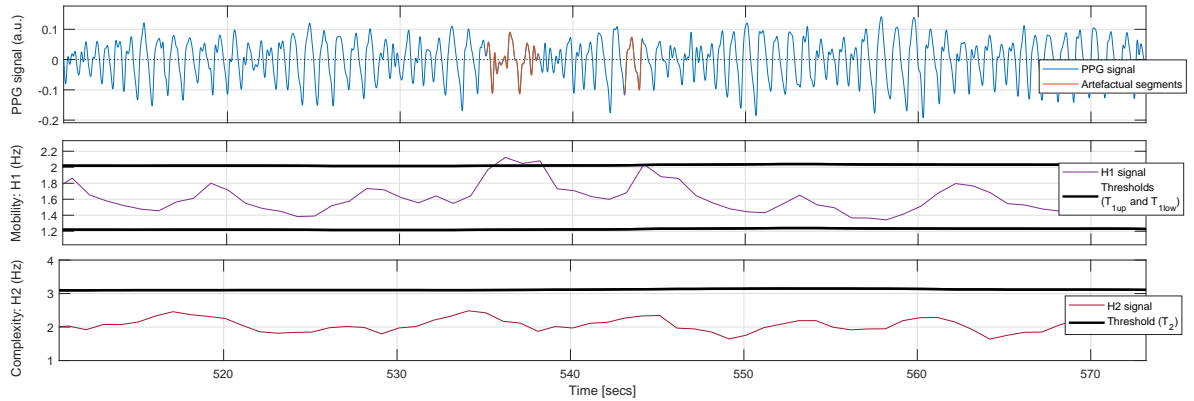
FIGURE 2.1: *Artefact Detection based on Hjorth Parameters.*

However, the artefactual segments of the PPG at the forehead had by far much more energy than good-quality signal segments and Hjorth parameters didn't work properly in this case "as was". In order to solve this problem, a PPG artefact detector based on the energy of the signal was implemented, assuming that a motion artefact has much more energy than the normal PPG signal (see red segment in Figure 2.2 (a)). The automatic detection of the high-energy artefactual segments is made following these steps:

1. The variance of the squared PPG signal -in order to emphasize the artefact segments- is calculated in a 2 seconds sliding-window.

2. The threshold is calculated as the moving median of the result obtained in 1 with a 100 seconds sliding-window.

3. Sample to sample, when the value obtained in 1 is five times greater than the value obtained in 2, the sample is considered as artefact.

The thresholds were defined empirically as with Hjorth parameters. A representative example of the algorithm performance can be seen in Figure 2.2.
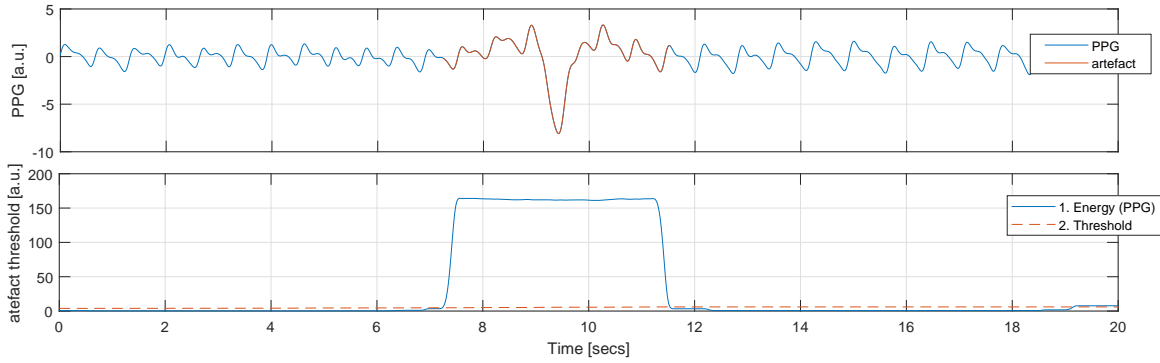

FIGURE 2.2: *Artefact Detection based on the power of the signal. (top) PPG signal where artefactual segments were defined, (bottom) Decision criteria.*

After the energy-based artefact detector, Hjorth parameters artefact detector was applied again. Some artefacts were actually detected and discarded, though some tiny artefacts affecting just morphology remained in the "cleaned" signal. The detected artefactual segments were excluded from the analysis.

2.2.2 Pulse detection

Subsequently to the preprocessing of the PPG signals, each PPG pulse was detected by an automatic pulse detector using the method developed in Lázaro et al. [49]. This algorithm detects the maximum upslope point of each PPG pulse (n_A^*) based on a low pass differentiator filter and time-varying threshold. Then, four FPs were computed: apex (n_A), middle-amplitude (n_M) and basal or foot (n_B) all of them defined based on the PPG pulse apex of the derivative PPG signal (n_A^*). The perfomance of n_M, n_B and n_A^* against artefacts is studied. The performance of nA is excluded from the analysis as it has been already reported that fluctuations around the apex of each pulse deteriorates the accurate pulse detection [46].

Briefly explained, the peak detection is performed based on the first derivative of PPG ($x'_{PPG}(n)$) using a time varying threshold which decreases gradually until a new pulse is detected, time at which $x'_{PPG}(n)$ overpasses the threshold. This threshold keeps the value of the detected pulse during a refractory period (150 ms). After this, it begins to decrease linearly. The whole algorithm is explained in [49].

For the maximum points detection, in order to better suit the smoother shapes of the PPG signals and for a greater robustness under artefactual conditions, the apex points n_A were set at the maximum point of the PPG pulses within a $\tau_A = \tau_B = 150$ ms-window, defined empirically, beginning at each peak $n_{A_i}^*$:

$$n_{A_i} = \underset{n \, \epsilon \, [n_{A_i}^* \, , \, n_{A_i}^* + \tau_A \cdot f_s]}{arg \, max} \{ \, x_{PPG}(n) \, \} \tag{2.1}$$

where $x_{PPG}(n)$ corresponds to the PPG signal. Then, the basal points of the PPG pulses, n_B, were set as the minimum points of the PPG pulses within a 150 ms window ending at each n_A^*:

$$n_{B_i} = \underset{n \, \epsilon \, [n_{A_i}^* \, - \, \tau_B \cdot f_s \, , \, n_{A_i}^*]}{arg \, min} \{ \, x_{PPG}(n) \, \} \tag{2.2}$$

The PPG pulses middle-amplitude points n_M were set as the point between n_A and n_B where the amplitude has reached 50% of the maximum of the pulse amplitude:

$$n_{M_i} = \underset{n \, \epsilon \, [n_{B_i} \, , \, n_{A_i}]}{arg \, min} \left\{ \left| \, x_{PPG}(n) - \frac{x_{PPG}(n_{A_i}) + x_{PPG}(n_{B_i})}{2} \, \right| \right\} \tag{2.3}$$

When either the maximum or the minimum FP cannot be defined, no pulse detection is considered for any of the FPs but the $n_{A_i}^*$. In this work, the FPs n_B, n_A^* and n_M were used for the robustness analysis.

The points of the i_{th} PPG pulse computed for PAT analysis are shown in Figure 2.3 for both forehead and finger PPG signals as well as the R-waves detected for the i_{th} ECG beat as reference.
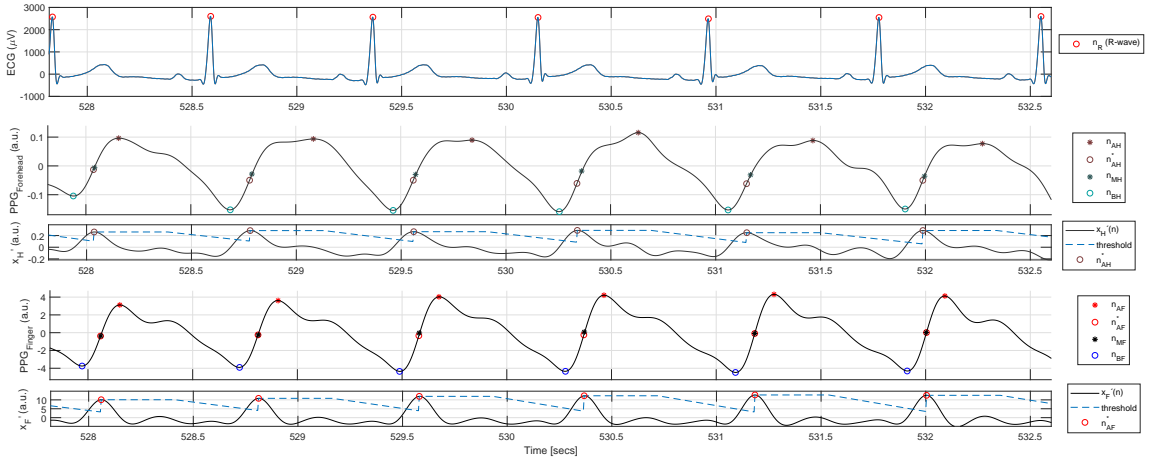

FIGURE 2.3: *Delineation in ECG [50] and PPG [49] signals.*

2.2.3 Pulse post-process

This stage was implemented in order to correct wrong- or miss-detections and let them vary only within a physiological range. The spurious detections were eliminated by means of an

"outlier" detector with the parameters adjusted empirically [51], in order to avoid as far as possible erroneous detections. Such outlier estimates are detected when the absolute value of the PAT or PTTD estimates exceeds a threshold $\eta(t_i)$. The threshold $\eta(t_i)$ is defined as the running standard deviation of the $N_e = 10$ most recent estimates, multiplied by a factor $C = 2.75$. For $i < N_e$, $\eta(t_i)$ is computed from the available estimates. When a value is out of boundaries, it is plotted in red and is suppressed for the analysis.
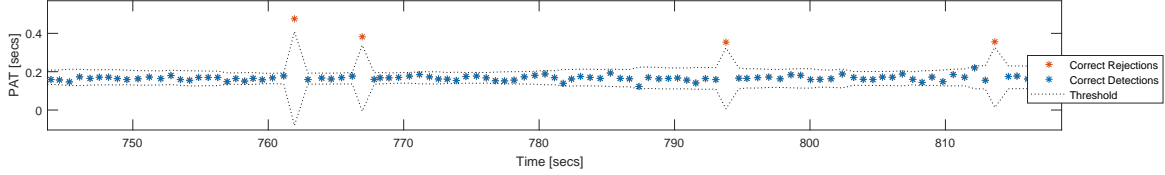

FIGURE 2.4: *Outlier Rejection at PAT signals [51].*

After that, the algorithms developed by Mateo et al. [14], to eliminate ectopic beats and erroneous detections in the QRS occurrence at the ECG for robust HRV analysis, were adapted for the detections of the PPG pulses at forehead and finger (shown in Figure 2.5).
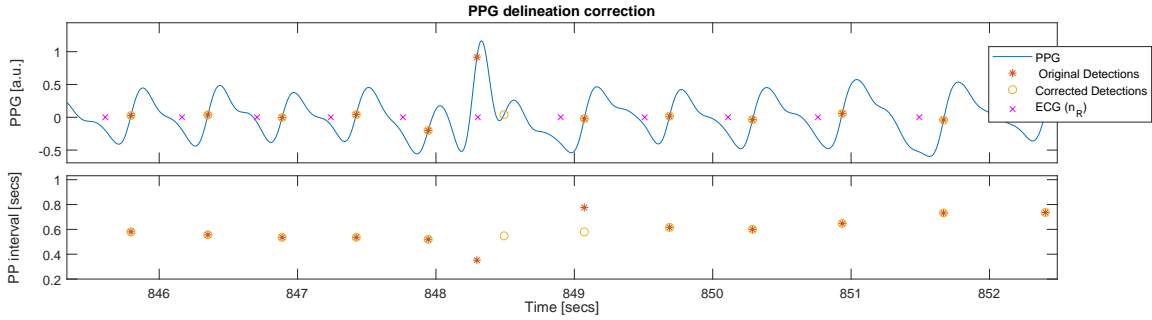

FIGURE 2.5: *Correction by Heart Rythm of the PPG pulse detections [14].*

2.2.4 PAT and PTTD computation

The pulse detection stage included the automatic QRS detection from the ECG signal using a wavelet-based ECG delineator [50], to use the ECG pulse definition as reference for the PAT definition. The heart beats were detected from the "X" lead of the recorded orthogonal ECG signal sampled at 1000 Hz. The maximum of the R waves are considered as the beat time instants and denoted as n_{Ri}, or also t_{k_i} in other studies, for the *i-th* beat index.

The FP chosen for the PPG signals were the maximum-amplitude point in the first derivative ($n^*_{AF_i}$ for the finger and $n^*_{AH_i}$ for the forehead PPG signals), the basal point (n_{BF_i} and n_{BH_i}) and the middle amplitude point (n_{MF_i} and n_{MH_i}). Theoretical definitions of $PATF$, $PATH$, and $PTTD$ were illustrated in Fig. 1.10.

PAT was measured as the difference of those FPs detected at the finger-PPG signal and those detected in the ECG signal:

$$x^u_{PATF}\left(n^*_{AF_i}\right) \;=\; \left[n^*_{AF_i} - n_{R_i}\right] \;\cdot\; \delta(n^*_{AF_i}) \tag{2.4}$$

where the superscript "u" denotes that the signal is unevenly sampled . Similarly, $x^u_{PATH}(n^*_{AH_i})$ was computed as the difference of $n^*_{AH_i}$ and n_{R_i}. The reference for both PATs is the ECG, defined in the n_R series.
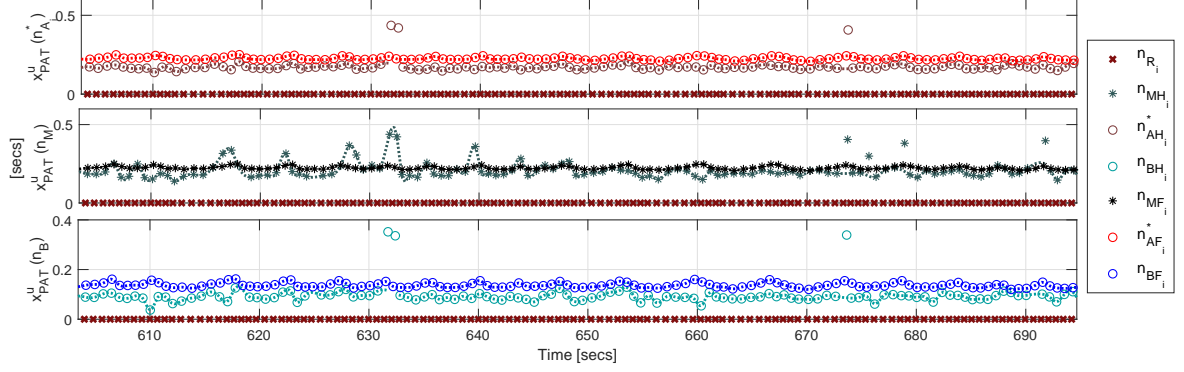

FIGURE 2.6: *Computed PAT plot. Dotted lines correspond to the evenly interpolated versions (see 3.2.1). The ECG detections are represented with a garnet cross as reference.*

As the finger and forehead PAT are affected by the same PEP, the PTTD can be measured as the PAT difference or, likewise, the pulse instant difference, i.e.:

$$x^u_{PTTD}(n^*_{AF_i}) = [n^*_{AF_i} - n_{H_i}] \cdot \delta(n^*_{AF_i}) \tag{2.5}$$

Note that the pulse detections at finger are considered as the reference of the PTTD, i.e. the PTTD pulses are defined on the finger definition instants. Some considerations for the equation 2.5 are:

- A pulse $x^u_{PTTD}(n^*_{AF_i})$ is considered not valid if the result of the difference is bigger that 150 ms or lower than -50 ms. If any difference between $n^*_{AF_i}$ and $n^*_{AH_i}$ is out of these bounds, that i_{th} pulse is not considered within the physiological range and is omitted.
- The PPG detections at finger, i.e. the n^*_{AF} pulses, are considered as the reference because of its reliability and common use rather than $n^*_{AH_i}$.
- $x^u_{PTTD}(n^*_{AF_i})$ can be negative, i.e. the pulse gets finger sooner than forehead.

Some miss-detection in PTTD arrive in next to the $2th$, $4th$, $5th$ and $6th$ heart beats (n_{Ri}). For example, around the second 962 there is a beat ($4th$ PPG finger beat) but PTTD cannot be computed because $t(n^*_{AF_4} - n^*_{AH_6}) > 150ms$. Also, one can notice that the $6th$ PTTD pulse seems to be negative.

2.2.5 Statistical Test

To evaluate the performance of each FP on capturing the similar variations from different PPG signals, the variance of x^u_{PATF} (σ_{PATF}) and the variance of PATH (σ_{PATH}) is calculated; then the feature $\Delta\sigma = \sigma_{PATF} - \sigma_{PATH}$ is introduced to quantify the changes in the variance. If PATs had a similar variance, $\Delta\sigma$ would be close to zero, while the presence of artefacts introduces variations in PATs which can result in higher values of $\Delta\sigma$.
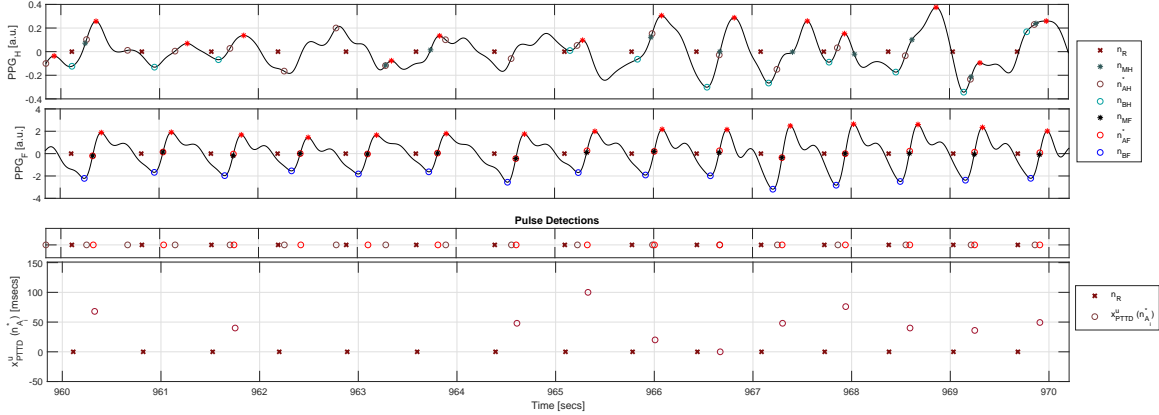
FIGURE 2.7: *PTTD plot for each FP. The considerations explained below can be seen in this extract of signal. Each garnet cross stands for a heartbeat.*

To reduce the contribution of outliers on the variance estimate, first the variance is calculated in a sliding window of 60 seconds pulse-by-pulse. Afterwards, the variance that characterize each series (σ_{PATF}, σ_{PATH}) is defined as the median value of all these short-term variance estimates.

A paired statistical test for each subject (14 in total) is used to evaluate whether the $\Delta\sigma$ distributions for different FPs differ in order to study the robustness of each FP against residual artefacts in the present database.

And so, the statistical tests used here are the Kolmogorov-Smirnoff test and the Wilcoxon signed-rank test. On the one hand, the Kolmogorov-Smirnoff test is performed in order to quantify the normality of the distributions. On the other hand, the paired sample Wilcoxon signed-rank test is a non-parametric method used in the comparison of the equality of the medians for two populations especially when the normality assumption of the data is violated.

$$H_0: \text{equal medians}$$
$$\text{if } p - value < 0.05: \text{reject } H_0$$

2.3   Results

Qualitative results given by an eye exploration of diverse PPG, PAT and PTTD signals underwent that n_A^* or n_B had much less error over n_M due to the bad quality of the PPG forehead signals. However, a statistical analysis is necessary to quantify the errors and conclude with numerical arguments.

The PPG in the figure 2.8 is an example of the PPG signals at forehead and at finger. The forehead signals have the dicrotic notch too much accentuated leading to badly-defined detections in n_A, hence affecting n_M. In this extract of signal, the threshold defined in the first derivative

to detect pulses (blue dashed lines in Fig. 2.8) avoids some dicrotic pulses that could have been considered as detections if we simply looked for local maxima at the first derivative.
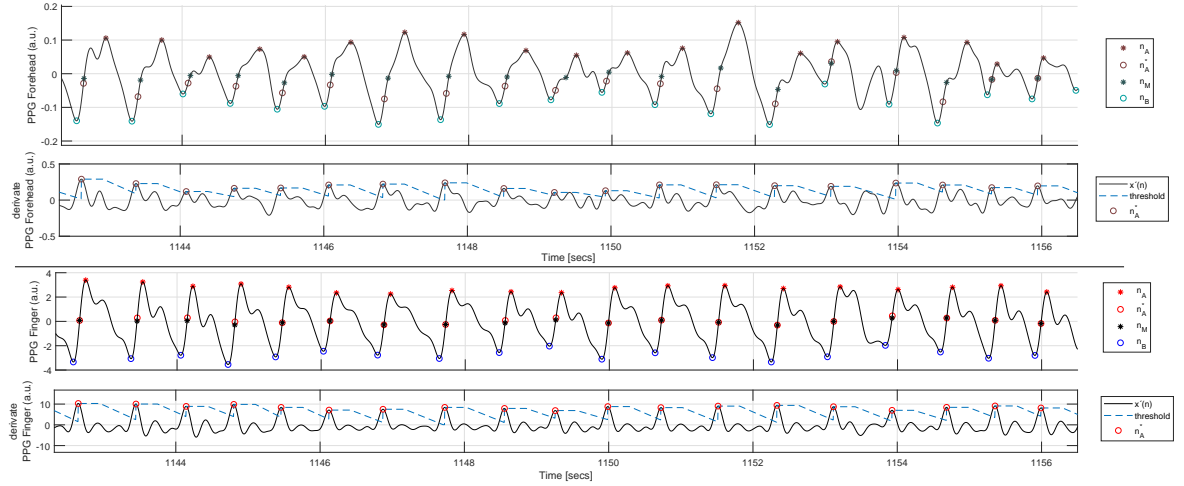

FIGURE 2.8: *PPG and detections at forehead (a) and at finger (b) for one subject.*

Looking at the histograms for two representative subjects (Figures 2.9 and 2.10), the distribution along n_M at forehead is skewed to the right side, making its standard deviation much bigger compared with the other FPs at the same location (in forehead distributions). Moreover, the outliers in each distribution (see the corresponding top plots and the corrected distributions in the bottom) are seen to be corrected when using n_A^* or n_B, but not with n_M. This effect can also be seen like, with n_A^* or n_B as FP, the PAT distribution regarding finger and forehead are visually separable into 2 different distributions, but not with n_M.

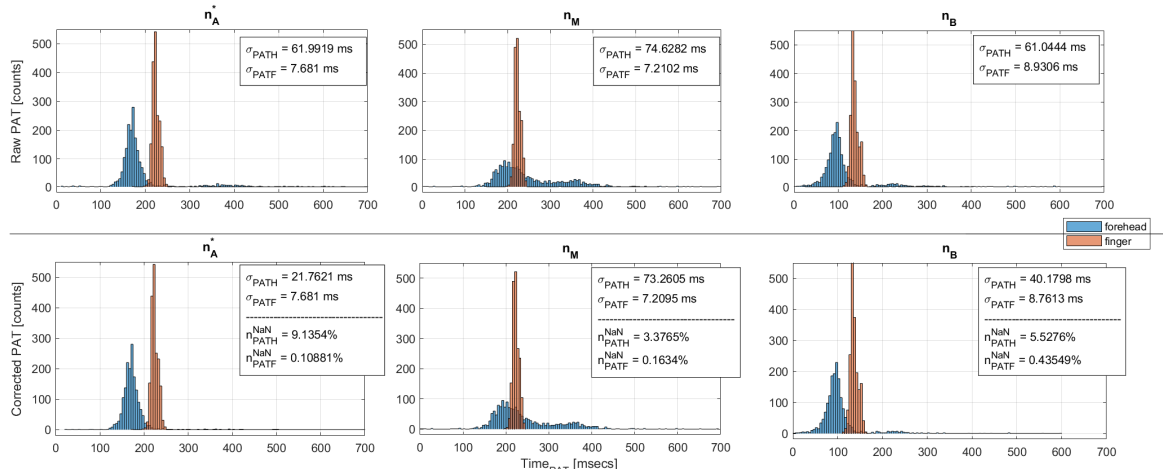FIGURE 2.9: *Probability Density Distribution for the different FPs "raw" (top) and corrected (bottom). Subject 17.*

Also, it is noticeable that the correction made by the whole post-process (corresponding to the bottom part on Figures 2.9 and 2.10) made the standard deviation of the forehead distribution, where the presence of artefacts is more frequent, decrease heavily. The n^{NaN} stands for the
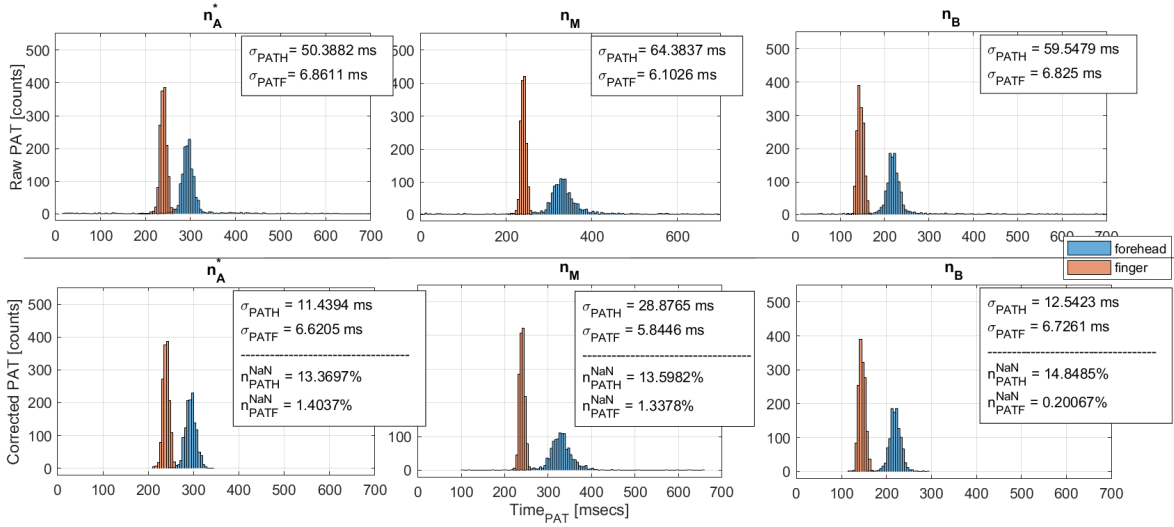
FIGURE 2.10: *Probability Density Distribution for the different FPs "raw" (top) and corrected (bottom). Subject 37.*

percentage of the PAT measures that couldn't be defined or were discarded in post-processing with respect to the total number of ECG heartbeats.

It is important to highlight that, from the total database, 40 subjects have been analysed up to now but only 14 subjects had both PPG signals with sufficient quality to be able to calculate the corresponding PTTD with a detection percentage n^{NaN} greater than 70% with respect to the number of heartbeats.

The difference of the standard deviation between finger and forehead for each FP and 14 subjects was computed. According to the result of the Kolmogorov-Smirnoff test, none of the distributions followed a normal and symmetric distribution ($p > 0.05$). Therefore, the Wilcoxon paired test was performed in order to see if there were statistically significant differences among FPs:

	n_A^* vs n_M	n_B vs n_M	n_A^* vs n_B
$\Delta\sigma$	**0.00024***	0.0580	0.8077

TABLE 2.1: *p-values comparing standard deviation in PAT and PTTD.*

Significant differences ($p < 0.05$) were found for the $\Delta\sigma$ distributions between the FPs n_M and n_A^*. A high variation in the PAT values is noticed when PATs were calculated from the PPG signals using the medium point, n_M, as FP. The difference in the PATs variance, quantified by $\Delta\sigma$, using n_A^* as FP was significantly lower suggesting that n_A^* is more robust in the presence of artefacts. Moreover, no statistical differences were found between n_A^* and n_B. This can be seen also visually in the kurtosis and skewness of the histograms: when computing PATH with n_A^* or n_B as FP, the distribution is less tailed and more centred to the median unlike when computing PATH with n_M.
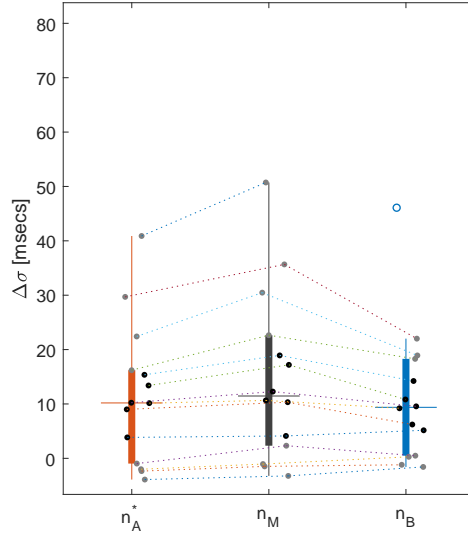
FIGURE 2.11: *Boxplot of standard deviations for (a) PAT and (b) PTTD.*

2.4 Discussion

The variance of the PAT series (PATH and PATF) for PPGs recorded at different distances to the heart (forehead and finger) were calculated. The effect of PEP must be the same for both type of PAT since they are defined based on the R-wave position of the ECG and both PATs should have similar variance induced by the different variations in the PTT; as consequence a low $\Delta\sigma$. In artefact presence and with non-stable PPG morphologies higher values of $\Delta\sigma$ were observed. Results showed that n_A^* had statistically significant lower $\Delta\sigma$ than n_M ($p < 0.05$) suggesting that n_A^* might be more robust to the presence of artefacts or changes in morphology. On the other hand, no statistical differences were found between n_A^* and n_B suggesting that they had a similar performance.

The boxplot in Figure 2.11 illustrates the distribution of $\Delta\sigma$ for the three FPs. When the detections are well-defined (considered as lowest standard deviations and peaky distributions), the three FPs have a good performance, but if the quantity of artefacts increases, the detections become worse in n_M than in n_A^* or n_B.

In the present database, the bad positioning of the PPG sensor at forehead introduced artefacts in the PPG morphology. It has been reported that the forehead PPG signals can provide reliable information under non-stationary conditions [48] and thus, their analysis is of particular interest in the present database even though the signal quality was low in some segments. The apex pulse definition, n_A, resulted to be less robust because of the dicrotic notch, which turned out to have the greatest amplitude in many PPG pulses at forehead as shown in Figure 2.8. So, it should be noted that as n_M depends on the precision of n_B and n_A, an error occurs in n_M if one of the others cannot have been delineated properly.

The most accurate point in [48], for PRV analysis in non-stationary environments, was the

midpoint n_M, although the precision of n_A^* was quite similar. In fact, in Rajala et al. [46] the apex point of the first derivative n_A^* was considered the most promising FP to be used in PAT. Hemon and Phillips [52] found the first PPG derivative method to be the best method for PRV analysis as well, after the intersecting tangent method between n_B and n_A^*.

Nonetheless, although the results using the value at the first derivate, n_A^*, as FP seemed promising, it might not be always the best choice to detect the PPG pulses. In fact, a robustness analysis should be made for each database to ensure reliability, performing simulation studies based on PPG pulses which account for morphological variations suitable for each particular application. For example, when using a database were young subjects are registered, it is probably worth using the basal point, n_B, instead of others because the bottom shape is very well-defined in them, despite here n_A^* worked better for this database. As reference, Mukkamala et al. [7] reported the typical range from 180 ms to 260 ms for PAT calculated with the basal point, n_B. Similar values are reported in this study but in some cases bigger variations can be attributed to the window threshold used to compute the PTTD ([-50,150] ms-window). This fixed threshold should become adaptive to the pulse rate, which means that the length of the time-window would change in the same way as the heart rate.

As the PPG pulse wave morphology changes in this database, other methods less sensitive to morphology for the pulse detection (like those based on mass centre) were considered at the beginning of the project, taking into account that the robustness of the FP on PPG is important for the analysis. However, the performance was not higher than the obtained with the purposed methodology (using n_A^* as FP).

Apart from the artefact detectors developed (see Section 2.2.1), an artefact detector based on neural networks and pattern recognition (Self-Organizing Map) was also implemented. Had any improvement been achieved with respect to the detectors shown in this work, the method would have been further investigated and could have been used as another artefact detector, but the performance was similar. Nevertheless, this method figured out that Principal Component Analysis (PCA) analysis was also useful for artefact detection. So, further studies to implement PCA within the current artefact detector could be made.

The issue regarding that only 14 subjects with an acceptable percentage of detections were extracted from the database used is because many artefacts appeared in the PPG recorded at forehead as it was not registered properly. It results necessary to clarify that there are dedicated techniques and sensors with the focus of measuring PPG in the forehead that could implement the PTTD technique in a very reliable way.

2.5 Conclusions

The most promising FP to be used in PAT or PTTD calculation is the apex of the first derivative of the PPG (n_A^*), since it provides the lowest variance between PAT series, derived for the forehead and the finger PPG signals, and its computational complexity is very much lower than the rest of the FPs.

Stress Response and PTTD: A Proof of Concept

Contents

Unfortunately, the identification of stress is not trivial and there are only few methods to obtain a quantificable measure of it, mainly based on ECG, ElectroDermal Activity (EDA) and respiration parameters [4]. When stress is prolonged or repetitive, it has been associated with psychic and somatic diseases. Moreover, chronic stress has been related with higher risk of suffering cardiovascular diseases. Therefore, there is need to investigate methods towards an objective measure of stress.

PTTD has been used in previous studies as it is said to carry ANS-related information not influenced by PEP, which withdraws the non-invasively derivable cardiovascular features [45, 53]. As PTTD is strongly related with the time it takes for a pulse pressure wave to propagate along the arteries, the responses changing blood vessels' properties also influence its variation (such as vascular radius, compliance and thickness).

In this chapter, a new method to detect states of stress is presented, based on the PTTD. The hypothesis on which it is based on is that stress evokes an autonomous response, hence a change in vasoconstriction that reflects a change in the PWV, and as a consequence in PTT. PTTD is proposed here as a PTT surrogate to detect acute mental stress episodes.

3.1 Materials

3.1.1 Database

The database is the same as the previous chapter, but the stress-evoking protocol is going to be explained in the following. As said before, the protocol used was approved by the Ethics Committee and all the subjects volunteered to participate giving their informed consent before participating in the study. An observational and transversal study is used, explained entirely in [17] and analyzed on multiple occasions [4, 17, 54], where each individual was subjected first to normal and then in acute stress conditions.

The experimental protocol included two sessions, called basal and stress, which were carried out on different days and lasting approximately one hour (see Figure 3.1). In the first session, the individual's relaxation is induced, leading him to a state of Relax; in the second session, stress is induced by applying the stressful stimulus typified as Trier Social Stress Test (TSST) [55] with an additional arithmetic task, being at the end of the stress session when the individual reaches the state of greatest stress.

The basal session consisted of a 35 minutes-length relaxing audition and a state of autogenic relaxation is induced through an audio record. The first 10 minutes are considered as the subject's baseline resting state (BL_B) and in the next twenty-five minutes the subject is underwent to a state of relaxation (R). The stages of the stress session were ordered as follows:

i. Baseline stage during stress session (BL_S): A state of autogenic relaxation with a 10 minutes-length duration.

ii. Story-telling stage (ST): three stories are told to the subject with a great amount of details. The subject is requested to remember as much details as possible, demanding a great amount of attention. This one lasts approximately 2 minutes.

iii. Memory Test (MT): The subject is requested to tell back every remembered detail within 30 s for each story while he is recorded on video.

iv. Stress Anticipation (SA): The subject remains waiting 10 minutes for the evaluation of the previous task.

v. Video Exhibition (VE): a projection of a video with the subject performance in the memory test is shown. The video showed twice each one of the three stories. First, an actor repeats the story in a perfect way, trying to make the subject believe that his performance was unsatisfactory. Subsequently, the subject (recorded during the MT stage) telling back the story is displayed.

vi. Arithmetic Task (*AT*): The subject must perform the consecutive subtraction from 13 to 1022 and in case of a calculation error, the countdown starts again. Although the subject is not expected to complete the countdown, he is requested to do so within 5 min. Any subject completed the countdown.
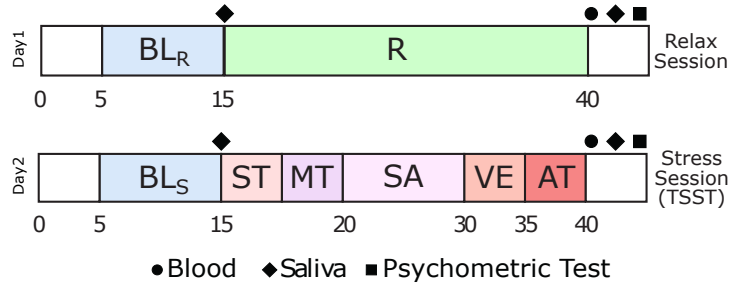

FIGURE 3.1: *Sessions of the experimental protocol [17]. BL_B: Basal Relax. R: Relax. BL_S: Basal Stress. ST: Story Telling. MT: Memory Test. SA: Stress Anticipation. VE: Video Exhibition. AT: Arithmetic Task.*

Just the last five stages of the stress session are considered stressful, being at the end of it when the individual reaches the greatest state of stress. In order to avoid possible transient phenomena in the different phases, the statistics were analysed using a 1 minute-length sliding window.

Note that the SA stage, in which the subject was waiting for the evaluation of the previous tasks there wasn't a specific stressor, in contrast to the stages of ST, VE or AT. Memory Task, MT, and Arithmetic Task ,AT, were not analysed due to the fact that the subjects were speaking and the physiological interpretation of the results is not straightforward.

3.2 Methods

In brief, the signal processing steps to obtain the PTTD signal are the following (explained previously in Section 2.2):

- Filtering and artefact detection.
- PPG and ECG pulse detection.
- Pulse correction and post-processing.
- PTTD computation.

According to the conclusions of the Chapter 2, the FP chosen for the analysis was the maximum point at the first derivative defined as the instant when the PPG pulse reaches the maximum slope. After that, a frequency analysis of the PTTD signal is performed for the physiological interpretation of the results in function of the SNA. Finally, a statistical analysis is used to study the capacity of the PTTD on quantifying ANS changes between relax (control/reference) and stress stages.

3.2.1 PTTD Spectral Analysis

Spectral analysis based on Heart rate variability (HRV) has been extensively studied as well as the physiological interpretation of its frequency components. However, few studies have analysed the spectral components of the PTTD signals. So, subsequently to the PAT and PTTD computation (sec. 2.2.4), in order to perform spectral estimation, the evenly-sampled versions of $x^u_{PATF}(n^*_{AF_i})$, $x^u_{PATH}(n^*_{AH_i})$, and $x^u_{PTTD}(n^*_{AF_i})$ were obtained by cubic spline interpolation, being denoted as $x_{PATH}(n)$, $x_{PATF}(n)$, and $x_{PTTD}(n)$, respectively.

As it has been explained in previous Chapter there exist gaps in the PATH and PTTD series whenever a segment was identified as an artefact or an estimate has been considered as an outlier. Then, PATH and PTTD series free of gaps longer than 2 seconds were interpolated at 4 Hz using cubic-spline interpolation. An example of these signals is shown in Fig. 3.2.
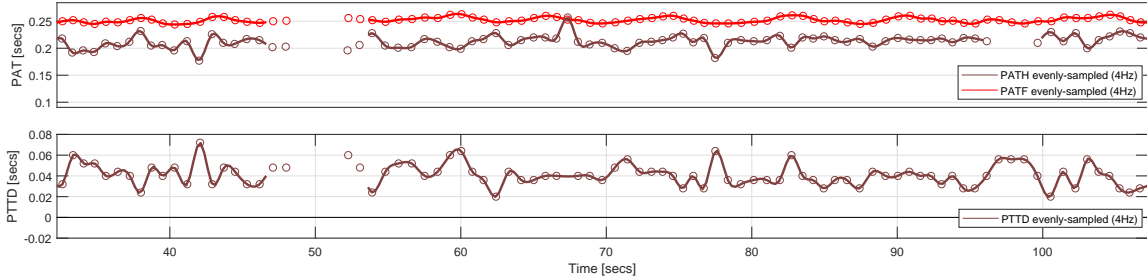

FIGURE 3.2: *Evenly-sampled versions of corrected PAT (a) and PTTD (b) by cubic spline interpolation.*

3.2.2 Statistical Test

The objective of this analysis is to find statistically significant differences in PTTD-based features between the stress (ST, VE, SA) and relax (BL_S) stages of the protocol.

The features used are the median and standard deviation of the unevenly sampled series of $x^u_{PTTD}(n^*_{AF_i})$ for the 14 subjects. Each feature is calculated as the median value of the beat-by-beat sliding window of 60 beats-length in order to avoid bias estimation when stages with different duration are analysed.

The Wilcoxon signed-rank test for each subject was performed to study the differences between basal and stress stages.

3.3 Results

All the PTTD signals computed are shown in Figure 3.3. The grey stars represent the corresponding PTTD detections for each subject and the coloured lines represent the corresponding evenly-sampled interpolated signals in the different stages of the protocol. Some gaps in the $x_{PTTD}(n)$ can be seen due to bad-detections of PPG pulses. Also, the figure accounts for the

completely different mean PTTD at different subjects, showing the high inter-subject variability in the PTTD. Note that the length in basal stage (approximately 8 minutes for BL_S) is much greater than the length of both stress stages (approximately 1 minute for ST and 2.5 minutes for VE) and thus, the sliding window to calculate the median and the variance was used.
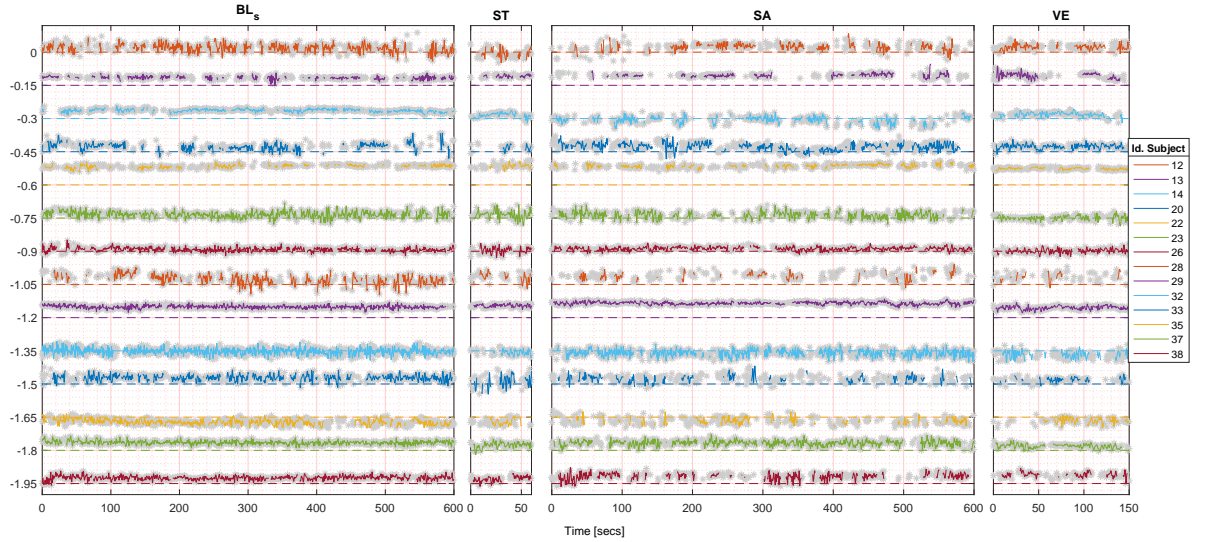
FIGURE 3.3: *PTTD in stages for all the subjects analysed.*

Figure 3.4 shows a boxplot diagram for the median and standard deviation of the PTTDs for all the subjects). Accordingly, Table 3.1 shows the p-values obtained by comparing the median and standard deviation of the PTTD among basal stage and the different stress stages of the protocol using the Wilcoxon test.
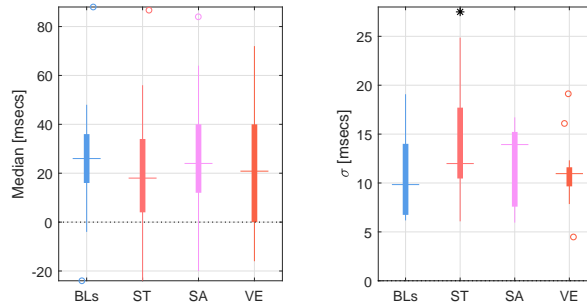
FIGURE 3.4: *Boxplot with (a) median (PTTD), (b) σ (PTTD). Te marker ∗ stands for significance difference with p < 0.05.*

Parameters	BL_S vs ST	BL_S vs SA	BL_S vs VE
Median	0.15	0.45	0.17
σ	**0.005***	0.10	0.76

TABLE 3.1: *P-values comparing PTTD between sessions.*

After that, the spectral analysis, in order to compute the frequency indices [15], couldn't be performed for all the subjects since the duration of the evenly-sampled PRV signals without

time gaps were too short to be done. In particular, only the PTTD spectra of four out of the
fourteen subjects could be analysed. An example of one of those is shown in Figure 3.5.

FIGURE 3.5: *PTTD spectral analysis for BL_S and ST stages. (top) HRV (from the ECG) with
Respiration, (bottom) PTTD, PATF and PATH spectral estimation.*

3.4   Discussion

In this study, a new method to detect states of stress based on the PTTD is presented. As shown
in Table 3.1 and in Figure 3.4, statistically significant differences for the variance of PTTD
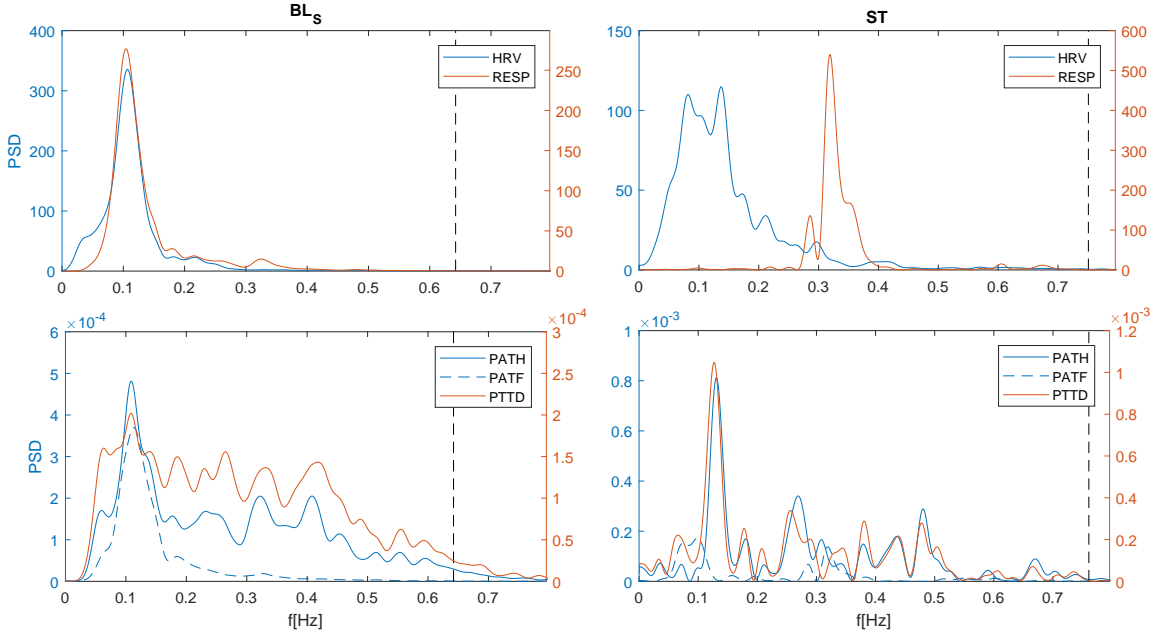were found in the ST when compared to BL_S, suggesting that it might be useful to detect
states of acute mental stress. Although there were no statistically significant differences in the
median -that could be due to the small number of subjects-, a descending trend is observed
in the stressful stage ST compared to the relax stage BL_S. On the other hand, no significant
differences were found in VE and SA, perhaps due to the absence of a specific stressor as in
ST.

As explained and discussed in the previous chapter, only 14 subjects had both PPG signals with
sufficient quality to be able to calculate the corresponding PTTD with a detection percentage
greater than 70% with respect to the number of heartbeats. Only the basal stage of the stress
session (BL_S) is used here as relax-reference since the stages BL_B, R and BL_S were shown to
be highly similar in previous studies [4, 17]. Furthermore, AT stage was discarded from the
analysis since the physiological interpretation of the results becomes difficult when a subject is
speaking.

In a SNS activation, a large vasoconstriction occurs in the arterioles and therefore, according

to the Continuity principle, an increase in the PWV. However, when a SNS activation occurs, vasoconstriction is greater in the arterioles of the peripheral system (such as in the finger) than in arterioles near the central nervous system (such as in the forehead) due to physiological necessities. Then, the PWV towards the finger will increase to a greater extent than the PWV towards the forehead causing the mean PTTD to decrease. Nonetheless, although the results obtained (see Figure 3.4) seem to go in that direction, there is not enough data to firmly support this hypothesis. Further studies should be conducted in order to investigate the descending trend of the PTTD in stress-mediated activations.

Higher values of σ in ST compared to BL_S might be also related to the differences in the local vasoconstrictions since affect PPG morphology in a different manner depending on the aquisition site in the human body. In a relax stage, vasoconstriction can be similar to the head and to the finger, but in a stressful stimulus it can vary more in the extremities that are affected by the SNS. Shelley et al [56] reported indeed that the respiratory signal in the pulse-oximeter waveform was more than 10 times stronger in the region of the head when compared with the finger. This leads to think that the vasculature of the head is relatively insensitive to local sympathetically mediated vasoconstriction that may mask respiration-generated oscillations, suggesting that under a stressful situation higher variations in PTTD might be associated to the higher differences between the morphological variability of different PPG signals recorded at different sites of the body.

The usage of different FPs to define the PTTD and the complex interplay with various physiological modulations in PPG could affect the interpretation of the results. Fluctuations in PTT, HR, and BP may result from different interactions of the respective autonomic controls because cardiovascular system is maintained by a complex control loop. For instance, PTT varies inversely with pressure and thus it is expected that, during the respiratory cycle, it will vary cyclically with the pressure changes induced by respiratory activity. This is that, during inhalation, the arterial blood pressure reduces in the arterial tree, and hence transit time is expected to increase. Correspondingly, during exhalation, when the blood pressure increases, the transit time is expected to decrease [53].

The peripheral arterial pressure pulse is a superposition of several individual component pressure pulses, the first and more important one is due to the left ventricular ejection from the heart [57]. In this study the apex of the PPG first derivative, which correponds to the upslope of the initial pulse wave component, has been selected. This FP is related to the moment in which the systolic pulse wave reaches the highest velocity throughout the corresponding vessel. However, as mentioned before, PPG morphology contains strong respiratory modulations. In fact, in Lázaro et al. [58] the variations in slope transit time are used to retrieve respiratory information. As the transit time decreases, the gradient of the upslope of the initial pulse wave component should increase [53].

The above mentioned mechanisms imply that variations in PTTD could be partially related

to respiration which might be useful in stress application since respiratory information has been previously used to discriminate stress stages [4]. The mechanical effect of breathing in the stress phase may affect the PPG morphology differently than it does in basal. For instance, thoracic respiration, usually seen under stress activation, produces an increase in the blood flow velocity in the superior vena cava during inspiration whereas in abdominal respiration, usually seen in relax conditions, only a slight and transient increase in superior vena cava flow is seen during expiration [59]. The greater flow variations in thoracic breathing, compared with abdominal breathing, would result in significant respiratory-induced strong fluctuations in the PTTD signal. On the other hand, the respiratory frequency affects the respiratory component in the systolic blood pressure variation, with the greatest impact at lower respiratory rates [59].

Although the analysis of the results could only be computed on the median and the standard deviation, they show that the PTTD has the potential to detect mental stress. Then, further studies with a dedicated database must be conducted in order to compute an appropriate PTTD variability analysis and focus on the correlation of the PTTD variability, the PRV and the HRV. Following this line, Ma et al. [60] concluded that PTT variability is mainly caused by PNS regulations and significantly coupled with HRV and BP variability at HF.

3.5   Conclusions

The standard deviation of the PTTD is able to detect physiological states of stress by quantifying changes in the PWV. The high morphological variations induced by changes in breathing pattern and local vasoconstrictions in the PPG signals, recorded at different sites of the body, when a SNS activation occurs could explain the significant strong fluctuations in the PTTD signal.

Preliminary results of this chapter were presented at "*Congreso Anual de la Sociedad Española de Ingeniería Biomédica*" (CASEIB-2018, 19th-23rd of November) congress:

> P. Armañac, S. Kontaxis, J. Lázaro, P. Laguna, R. Bailón, E. Gil (2018). "Cambios en la Diferencia del Tiempo de Tránsito del Pulso Sanguíneo en Estados de Estrés Emocional Agudo". *XXXVI Congreso Anual de la Sociedad española de Ingeniería Biomédica (CASEIB18)*.

Conclusions and Future Work

T his chapter summarizes the original contributions and main conclusions of the project, and proposes possible extensions of the work.

4.1 Summary and Conclusions

As stated in the Introduction 1, the objective of this project was to study the possibility of quantifying changes in the sympathovagal balance caused by acute mental stress, using non-invasive sensors based on PPG and without the need of either the ECG or cuff/intra-arterial BP sensors. Prior to that, as the delineation of the PPG pulses was challenging, we needed to develop an artefact detector and a post-process method to correct the pulses series so that we could extract robust series of PAT and PTTD.

As concluded in chapter 2, the most promising FP to be used in PAT or PTTD calculation is the apex of the first derivative of the PPG (n_A^*), since it provides the lowest variance between PAT series, derived for the forehead and the finger PPG signals, and its computational complexity is very much lower than the rest of the FPs.

On the other side, it can be concluded that the standard deviation of the PTTD is able to detect physiological states of stress by quantifying changes in the PWV. The high morphological variations induced by changes in breathing pattern and local vasoconstrictions in the PPG signals, recorded at different sites of the body, when a SNS activation arise could explain the significant strong fluctuations in the PTTD signal. In addition, a descending trend is also observed in the mean PTTD when this stress-mediated activation of the SNS occurs.

4.2   Future Work

In this manuscript, some topics which may be used as starting point for further analysis have been described. Possible research lines to directly expand the work of this project are presented below.

- The defined values of PTTD physiological constrains ([-50,150] ms-window) should become adaptive to the pulse rate, which means that the limits of the time-window would change in the same way as the heart rate.
- Development of a MultiLayer-Perceptron Neural Network for artefact rejection. Using a database containing different patterns of labelled PPG pulses, it is possible to implement an automatic mechanism to accurately reject artefactual PPG intervals. Even further, using signal reconstruction techniques based on PCA, Wavelet transform or Gaussian models, those intervals could be corrected and become useful for analysis.
- Simulation study of the morphology of the PPG signal, using a physiological based model [61].
- Register a database with a multimodal approach:
  - Measure the PEP in order to be able to separate PEP and PTT effect from PAT.
  - Check whether PTTD is a good surrogate of the PTT not affected by PEP and consequently obtain their relationship.
  - Accurately measure the PTTD signal by recording high quality PPG-signals at 1000 Hz in order to obtain a less quantified PTTD (with 250 Hz the quantification is 0.08 msecs).
  - PRV and HRV correlation between PAT, PTTD and PEP to get a complete physiological interpretation of the PTTD.
  - PTTD measuring techniques: conclude which is the best PPG sensors disposal for PTTD estimation.

Though the next logic step would seem to be the robust detection of stress with the PTTD approach and the improvement of the stress assessment, other indirect lines to explore are not centred on signal processing. The development of a wearable device with both PPG and EDA (also known as Galvanic Skin Response (GSR)) sensors integrated and implemented in a minimal ring would be of interest as well.

The μController would be based on the nRF52832 chip, integrated in the EYSHSNZWZ module manufactured by TAIYO YUDEN. This Bluetooth®Low Energy Module is based on Bluetooth v5 and designed for space-constrained applications with an extremely small *3.25×8.55×0.9 mm* footprint. The module only requires DC power (3.6 V_{DC}) and operates on the 2.4 GHz band.

All the electronics are expected to be integrated into a wearable device capable of measuring EDA/GSR and PPG, connected to a smartphone or PC computer via Bluetooth v5. The connections would be made with Flex technology (see Fig. 4.2) in order to make the device
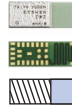
FIGURE 4.1: *TAIYO YUDEN EYSHSNZWZ Bluetooth® Low Energy Module* : *Real Size (1:1).*

easy of assembly and fabrication and give it the characteristic shape of a ring or wrist watch (see Fig. 4.3).
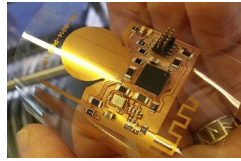

FIGURE 4.2: *Flexible Electronics.*

This kind of devices could also be helpful for other applications such as those developed in Lázaro et al. [58] to derive respiratory rate, or to assess cardiovascular health during everyday life. So this is a very important and interesting step to take into account for the development of an application to measure stress, moreover with the integration in the same device of the two more promising techniques for stress assessment.
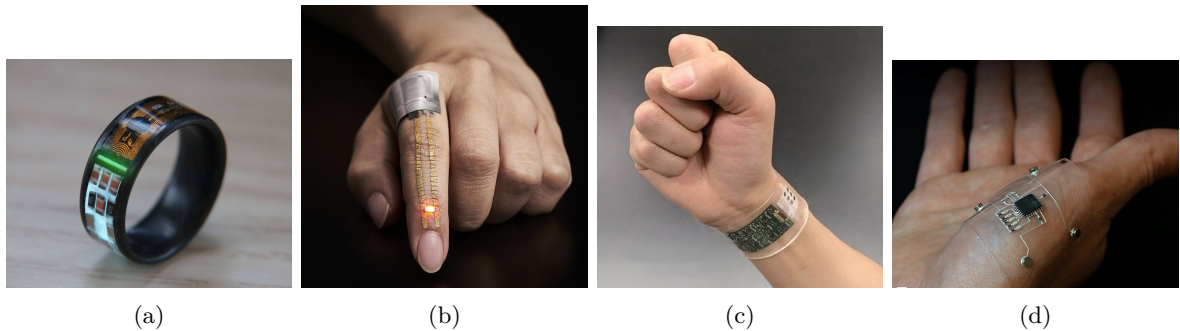
(a)   (b)   (c)   (d)

FIGURE 4.3: *Prototype for acquisition and communication with all electronics integrated. Some possible designs: (a) ring, (b) ring, (c) wristband, (d) palm-mounting.*

Bibliography

[1] Syed M Ahmed, Paul J Hershberger, and Jeanne P Lemkau.
Psychosocial influences on health.
Textbook of Family Medicine E-Book, page 24, 2011.

[2] Stavroula Leka, Amanda Griffiths, Tom Cox, World Health Organization, et al.
Work organisation and stress: systematic problem approaches for employers, managers and trade union representatives.
2003.

[3] Charalambos Vlachopoulos, Foteini Kosmopoulou, Nikolaos Alexopoulos, Nikolaos Ioakeimidis, Gerasimos Siasos, and Christodoulos Stefanadis.
Acute mental stress has a prolonged unfavorable effect on arterial stiffness and wave reflections.
Psychosomatic medicine, 68(2):231–237, 2006.

[4] Alberto Hernando, Jesús Lázaro, Eduardo Gil, Adriana Arza, Jorge Mario Garzón, Raúl López-Antón, Concepción de la Cámara, Pablo Laguna, Jordi Aguiló, and Raquel Bailón.
Inclusion of respiratory frequency information in heart rate variability analysis for stress assessment.
IEEE journal of biomedical and health informatics, 20(4):1016–1025, 2016.

[5] Robin P Smith, Jérôme Argod, Jean-Louis Pépin, and Patrick A Lévy.
Pulse transit time: an appraisal of potential clinical applications.
Thorax, 54(5):452–457, 1999.

[6] Xiao-Rong Ding, Yuan-Ting Zhang, Jing Liu, Wen-Xuan Dai, and Hon Ki Tsang.
Continuous cuffless blood pressure estimation using pulse transit time and photoplethysmogram intensity ratio.
IEEE Transactions on Biomedical Engineering, 63 (5):964–972, 2016.

[7] Ramakrishna Mukkamala, Jin-Oh Hahn, Omer T Inan, Lalit K Mestha, Chang-Sei Kim, Hakan Toreyin, and Survi Kyal.
Toward ubiquitous blood pressure monitoring via pulse transit time: theory and practice.
IEEE Trans. Biomed. Engineering, 62(8):1879–1901, 2015.

[8] Mico Yee-Man Wong, Carmen Chung-Yan Poon, and Yuan-Ting Zhang.
An evaluation of the cuffless blood pressure estimation based on pulse transit time technique: a half year study on normotensive subjects.
Cardiovascular Engineering, 9(1):32–38, 2009.

[9] W Chen, T Kobayashi, S Ichikawa, Y Takeuchi, and T Togawa.
Continuous estimation of systolic blood pressure using the pulse arrival time and intermittent calibration.
Medical and Biological Engineering and Computing, 38(5):569–574, 2000.

[10] Aman Gaurav, Maram Maheedhar, Vijay N Tiwari, and Rangavittal Narayanan.
Cuff-less ppg based continuous blood pressure monitoring—a smartphone based approach.
In *Engineering in Medicine and Biology Society (EMBC), 2016 IEEE 38th Annual International Conference of the*, pages 607–610. IEEE, 2016.

[11] Arthur Clifton Guyton, JE Hall, et al.
Textbook of medical physiology. philadelphia.
PA: WB Saunders Company, 2006.

[12] John M Karemaker.
An introduction into autonomic nervous function.
Physiological measurement, 38(5):R89, 2017.

[13] Dee Unglaub Silverthorn, William C Ober, Claire W Garrison, Andrew C Silverthorn, and Bruce R Johnson.
Human physiology: an integrated approach.
Pearson/Benjamin Cummings San Francisco, CA:, 2004.

[14] Javier Mateo and Pablo Laguna.
Analysis of heart rate variability in the presence of ectopic beats using the heart timing signal.
IEEE Transactions on Biomedical Engineering, 50 (3):334–343, 2003.

[15] AJMM Camm, Marek Malik, JTGB Bigger, Günter Breithardt, Sergio Cerutti, R Cohen, Philippe Coumel, E Fallen, H Kennedy, RE Kleiger, et al.
Heart rate variability: standards of measurement, physiological interpretation and clinical use. task force of the european society of cardiology and the north american society of pacing and electrophysiology.
Circulation, 93(5):1043–1065, 1996.

[16] Evangelia Charmandari, Constantine Tsigos, and George Chrousos.
Endocrinology of the stress response.
Annu. Rev. Physiol., 67:259–284, 2005.

[17] Jorge Mario Garzón-Rey and Jordi Aguiló.
Enfoque psicosomático de la medición de estrés.
PhD thesis, Universitat Autònoma de Barcelona, 2017.

[18] Hans Selye.
Stress and the general adaptation syndrome.
British medical journal, 1(4667):1383, 1950.

[19] Alrick B Hertzman.
The blood supply of various skin areas as estimated by the photoelectric plethysmograph.
American Journal of Physiology-Legacy Content, 124 (2):328–340, 1938.

[20] Abdullah Alzahrani, Sijung Hu, Vicente Azorin-Peris, Laura Barrett, Dale Esliger, Matthew Hayes, Shafique Akbare, Jérôme Achart, and Sylvain Kuoch.
A multi-channel opto-electronic sensor to accurately monitor heart rate against motion artefact during exercise.
Sensors, 15(10):25681–25702, 2015.

[21] John Allen and Alan Murray.
Age-related changes in the characteristics of the photoplethysmographic pulse shape at various body sites.
Physiological measurement, 24(2):297, 2003.

[22] John Allen.
Photoplethysmography and its application in clinical physiological measurement.
Physiological measurement, 28(3):R1, 2007.

[23] Yitzhak Mendelson.
Pulse oximetry: theory and applications for noninvasive monitoring.
Clinical chemistry, 38(9):1601–1607, 1992.

[24] Meir Nitzan, Anatoly Babchenko, Boris Khanokh, and David Landau.
The variability of the photoplethysmographic signal-a potential method for the evaluation of the autonomic nervous system.
Physiological measurement, 19(1):93, 1998.

[25] Eduardo Gil, José María Vergara, and Pablo Laguna.
Detection of decreases in the amplitude fluctuation of pulse photoplethysmography signal as indication of obstructive sleep apnea syndrome in children.
Biomedical Signal Processing and Control, 3(3):267–277, 2008.

[26] Eduardo Gil, MartÍn Mendez, JosÉ MarÍa Vergara, Sergio Cerutti, Anna Maria Bianchi, and Pablo Laguna.
Discrimination of sleep-apnea-related decreases in the amplitude fluctuations of ppg signal in children by hrv analysis.
IEEE Transactions on Biomedical Engineering, 56 (4):1005–1014, 2009.

[27] J Crighton Bramwell and Archibald Vivian Hill.
The velocity of pulse wave in man.
Proc. R. Soc. Lond. B, 93(652):298–306, 1922.

[28] Roland Asmar, Athanase Benetos, Jirar Topouchian, Pierre Laurent, Bruno Pannier, Anne-Marie Brisac, Ralph Target, and Bernard I Levy.
Assessment of arterial distensibility by automatic pulse wave velocity measurement: validation and clinical application studies.
Hypertension, 26(3):485–490, 1995.

[29] DJ Pitson et al.
Value of beat-to-beat blood pressure changes, detected by pulse transit time, in the management of the obstructive sleep apnoea/hypopnoea syndrome.
European Respiratory Journal, 12(3):685–692, 1998.

[30] Andrew Steptoe, Harold Smulyan, and Brian Gribbin.
Pulse wave velocity and blood pressure change: calibration and applications.
Psychophysiology, 13(5):488–493, 1976.

[31] David B Newlin and Robert W Levenson.
Pre-ejection period: Measuring beta-adrenergic influences upon the heart.
Psychophysiology, 16(6):546–552, 1979.

[32] David B Newlin.
Relationships ol pulse transmission times to pre-ejection period and blood pressure.
Psychophysiology, 18(3):316–321, 1981.

[33] AM Pichlmaier and M Schaldach.
Pre ejection period—pep as measure for the inotropic status of the heart.
In *Engineering in Medicine and Biology Society, 1992 14th Annual International Conference of the IEEE*, volume 2, pages 451–452. IEEE, 1992.

[34] Yoshihiro Sugo, Rie Tanaka, Takeshi Soma, H Kasuya, T Sasaki, T Sekiguchi, H Hosaka, and R Ochiai.
Comparison of the relationship between blood pressure and pulse wave transit times at different sites.
In *[Engineering in Medicine and Biology, 1999. 21st Annual Conference and the 1999 Annual Fall Meetring of the Biomedical Engineering Society] BMES/EMBS Conference, 1999. Proceedings of the First Joint*, volume 1, pages 222–vol. IEEE, 1999.

[35] RA Payne, CN Symeonides, DJ Webb, and SRJ Maxwell.
Pulse transit time measured from the ecg: an unreliable marker of beat-to-beat blood pressure.
Journal of Applied Physiology, 100(1):136–141, 2006.

[36] Guanqun Zhang, Mingwu Gao, Da Xu, N Bari Olivier, and Ramakrishna Mukkamala.
Pulse arrival time is not an adequate surrogate for pulse transit time as a marker of blood pressure.
Journal of applied physiology, 111(6):1681–1686, 2011.

[37] Arnold M Katz.
Physiology of the Heart.
Lippincott Williams & Wilkins, 2010.

[38] Jana Krohová, Barbora Czippelová, Zuzana Turianiková, Zuzana Lazarová, Ingrid Tonhajzerová, and Michal Javorka.
Preejection period as a sympathetic activity index: a role of confounding factors.
2017.

[39] J Muehlsteff, XL Aubert, and M Schuett.
Cuffless estimation of systolic blood pressure for short effort bicycle tests: the prominent role of the pre-ejection period.
In *Engineering in Medicine and Biology Society, 2006. EMBS'06. 28th Annual International Conference of the IEEE*, pages 5088–5092. IEEE, 2006.

[40] Mico Yee Man Wong, Emma Pickwell-MacPherson, Yuan Ting Zhang, and Jack CY Cheng.
The effects of pre-ejection period on post-exercise systolic blood pressure estimation using the pulse arrival time technique.
European journal of applied physiology, 111(1):135–144, 2011.

[41] Meir Nitzan, B Khanokh, and Y Slovik.
The difference in pulse transit time to the toe and finger measured by photoplethysmography.
Physiological measurement, 23(1):85, 2001.

[42] He Liu, Kamen Ivanov, Yadong Wang, and Lei Wang.
Toward a smartphone application for estimation of pulse transit time.
Sensors, 15(10):27303–27321, 2015.

[43] Claude Julien.
The enigma of mayer waves: facts and models.
Cardiovascular research, 70(1):12–21, 2006.

[44] CP Chua and C Heneghan.
Pulse transit time-derived respiratory parameters and their variability across sleep stages.
In *Engineering in Medicine and Biology Society, 2005. IEEE-EMBS 2005. 27th Annual International Conference of the*, pages 6153–6156. IEEE, 2006.

[45] Jesús Lázaro, Raquel Bailón, Pablo Laguna, Vaidotas Marozas, Andrius Rapalis, and Eduardo Gil.
Difference in pulse arrival time at forehead and at finger as a surrogate of pulse transit time.
In *Computing in Cardiology Conference (CinC), 2016*, pages 269–272. IEEE, 2016.

[46] Satu Rajala, Teemu Ahmaniemi, Harri Lindholm, and Tapio Taipalus.
Pulse arrival time (pat) measurement based on arm ecg and finger ppg signals-comparison of ppg feature detection methods for pat calculation.
In *Engineering in Medicine and Biology Society (EMBC), 2017 39th Annual International Conference of the IEEE*, pages 250–253. IEEE, 2017.

[47] Dilpreet Buxi, Jean-Michel Redouté, and Mehmet Rasit Yuce.
A survey on signals and systems in ambulatory blood pressure monitoring using pulse transit time.
Physiological measurement, 36(3):R1, 2015.

[48] Elena Peralta, Jesús Lázaro, Raquel Bailón, Vaidotas Marozas, and Eduardo Gil.
Optimal fiducial points for pulse rate variability analysis from forehead and finger ppg signals physiological measurement.
Physiological measurement, (under revision).

[49] Jesús Lázaro, Eduardo Gil, José María Vergara, and Pablo Laguna.
Pulse rate variability analysis for discrimination of sleep-apnea-related decreases in the amplitude fluctuations of pulse photoplethysmographic signal in children.
IEEE journal of biomedical and health informatics, 18(1):240–246, 2014.

[50] Juan Pablo Martínez, Rute Almeida, Salvador Olmos, Ana Paula Rocha, and Pablo Laguna.
A wavelet-based ecg delineator: evaluation on standard databases.
IEEE Transactions on biomedical engineering, 51(4): 570–581, 2004.

[51] Raquel Bailón, Leif Sornmo, and Pablo Laguna.
A robust method for ecg-based estimation of the respiratory frequency during stress testing.

IEEE transactions on biomedical engineering, 53(7): 1273–1285, 2006.

[52] Mathilde C Hemon and Justin P Phillips.
Comparison of foot finding methods for deriving instantaneous pulse rates from photoplethysmographic signals.
Journal of clinical monitoring and computing, 30(2): 157–168, 2016.

[53] Paul S Addison.
Slope transit time (stt): A pulse transit time proxy requiring only a single signal fiducial point.
IEEE Transactions on Biomedical Engineering, 63 (11):2441–2444, 2016.

[54] Spyridon Kontaxis, Jesús Lázaro, Alberto Hernando, Adriana Arza, Jorge Mario Garzón, Eduardo Gil, Pablo Laguna, Jordi Aguiló, and Raquel Bailón.
Mental stress detection using cardiorespiratory wavelet cross-bispectrum.
In *Computing in Cardiology Conference (CinC), 2016*, pages 725–728. IEEE, 2016.

[55] Juliane Hellhammer and Melanie Schubert.
The physiological response to trier social stress test relates to subjective measures of stress during but not before or after the test.
Psychoneuroendocrinology, 37(1):119–124, 2012.

[56] Kirk H Shelley, Denis H Jablonka, Aymen A Awad, Robert G Stout, Hoda Rezkanna, and David G Silverman.
What is the best site for measuring the effect of ventilation on the pulse oximeter waveform?
Anesthesia & Analgesia, 103(2):372–377, 2006.

[57] Martin C Baruch, Darren ER Warburton, Shannon SD Bredin, Anita Cote, David W Gerdt, and Charles M Adkins.
Pulse decomposition analysis of the digital arterial pulse during hemorrhage simulation.
Nonlinear biomedical physics, 5(1):1, 2011.

[58] Jesus Lázaro, Spyridon Kontaxis, Raquel Bailón, Pablo Laguna, and Eduardo Gil.
Respiratory rate derived from pulse photoplethysmographic signal by pulse decomposition analysis.
In *2018 40th Annual International Conference of the IEEE Engineering in Medicine and Biology Society (EMBC)*, pages 5282–5285. IEEE, 2018.

[59] Lena Nilsson, Anders Johansson, and Sigga Kalman.
Respiratory variations in the reflection mode photoplethysmographic signal. relationships to peripheral venous pressure.
Medical and Biological Engineering and Computing, 41(3):249–254, 2003.

[60] Heather T Ma and YT Zhang.
Spectral analysis of pulse transit time variability and its coherence with other cardiovascular variabilities.
In *Engineering in Medicine and Biology Society, 2006. EMBS'06. 28th Annual International Conference of the IEEE*, pages 6442–6445. IEEE, 2006.

[61] Swati Banerjee, Raquel Bailón, Jesus Lazáro, Vaidotas Marozas, Pablo Laguna, and Eduardo Gil.
A two step gaussian modelling to assess ppg morphological variability induced by psychological stress.
Computing, 44:1, 2017.